

Review

Optimization of Surface Properties of Plasma Electrolytic Oxidation Coating by Organic Additives: A Review

Mosab Kaseem ^{1,*} and Burak Dikici ² 

¹ Department of Nanotechnology and Advanced Materials Engineering, Sejong University, Seoul 05006, Korea

² Department of Metallurgical and Materials Engineering, Ataturk University, Erzurum 25240, Turkey; burakdikici@atauni.edu.tr

* Correspondence: mosabkaseem@sejong.ac.kr

Abstract: Plasma electrolytic oxidation (PEO) is an effective surface modification method for producing ceramic oxide layers on metals and their alloys. Although inorganic electrolytes are widely used in PEO, the organic additives have received considerable interest in the last decade due to their roles in improving the final voltage and controlling spark discharging, which lead to significant improvements in the performance of the obtained coatings. Therefore, this review summarized recent progress in the impacts of organic additives on the electrical response and the plasma discharges behavior during the PEO process. The detailed influence of organic additives, namely alcohols, organic acids, organic amines, organic acid salts, carbohydrate compounds, and surfactants on the corrosion behavior of PEO coatings is outlined. Finally, the future aspects and challenges that limit the industrial applications of PEO coating made in organic electrolytes are also highlighted.

Keywords: plasma electrolytic oxidation; soft plasma; organic additive; adsorption; corrosion



Citation: Kaseem, M.; Dikici, B. Optimization of Surface Properties of Plasma Electrolytic Oxidation Coating by Organic Additives: A Review. *Coatings* **2021**, *11*, 374. <https://doi.org/10.3390/coatings11040374>

Academic Editor: Qihua Fan

Received: 28 February 2021

Accepted: 22 March 2021

Published: 24 March 2021

Publisher's Note: MDPI stays neutral with regard to jurisdictional claims in published maps and institutional affiliations.



Copyright: © 2021 by the authors. Licensee MDPI, Basel, Switzerland. This article is an open access article distributed under the terms and conditions of the Creative Commons Attribution (CC BY) license (<https://creativecommons.org/licenses/by/4.0/>).

1. Introduction

Plasma electrolytic oxidation (PEO) is an effective coating method of valve metals to fabricate well-adherent oxide layers, which impart improved wear and corrosion performances in many aggressive environments [1–7]. The formation of PEO coatings is usually accompanied by a series of simultaneous events, such as acoustic emission, luminescence, and heat release, which are associated with a localized electric breakdown of the growing oxide layer [1]. Typically, the resultant PEO coating exhibited a large thickness up to ~200 μm depending on processing conditions, which certainly improves corrosion resistance [8]. Earlier works on PEO have reported that the surface properties of PEO coatings are mainly affected by the composition of the electrolyte, current mode, coating time, as well as the electrical parameters, namely, current density, current frequency, duty cycle, and cell potential [9–20]. Therefore, optimizing the processing parameters during PEO would be important as these parameters affect the characteristics of plasma discharges thereby, affecting the quality of the PEO coatings [1]. It should be pointed out that the modification of plasma discharges via the utilization of electrolyte composition has been in the spotlight since the combination of available elements generates many different compounds and potentially leads to different plasma behavior. Two major types of electrolytes are those containing organic compounds and those containing inorganic compounds [21–26]. While numerous investigations showed that organic compounds tend to be precluded in the coating layer during coating growth, the use of inorganic compounds generally showed successful incorporation [21].

PEO treatment as a kind of surface treatment of valve metals has previously been reviewed by several works [27–31]. For example, a critical review discussing the principle, structure, and performance of PEO coatings was reported recently by Kaseem et al. [1]. A review discussing the mechanism and performance of PEO-coated Mg alloys was documented by Darband et al. [27]. An interesting review very recently reported on micro-

discharge characteristics during PEO treatment [28]. The impacts of different particles on the characteristics of PEO coating have been reviewed by Lu et al. [30]. To date, however, the types of organic additives added to the electrolyte during PEO and their roles in fabricating compact coatings with improved protective properties have not been given sufficient attention. Therefore, this review discusses the incorporation of organic additives, their effects on the characteristics of plasma discharges, structure, and the corrosion performance of the PEO coatings. The pros and cons of each additive, challenges, and future aspects associated with these additives were also highlighted.

2. Influence of Organic Additive on the Electrical Response of PEO

Generally, organic additives tend to adsorb on the surface of metallic substrates during PEO treatment through their functional groups ($-\text{OH}$, $-\text{COOH}$, $-\text{NH}-\text{CO}-$, etc.), which would prevent the inorganic additives—the main components of the electrolyte—and dissolved oxygen from transferring to the anodic substrate, leading to easy increments in the cell voltage [32–37]. For example, Pak et al. [38] examined the influence of organic polar liquids, such as glycerol (GLY), triethanolamine (TEA), and 3-aminopropyltrimethoxysilane (APTMS) on the voltage-time response during PEO treatment of AZ31B Mg alloy. They reported that organic compounds interacted with the Mg surface through their $-\text{OH}$ groups, which separated the substrate surface from the electrolyte and increased the resistance of the coating. Similar findings were reported during PEO treatment of Mg alloys using other organic additives, such as starch [39,40], benzotriazole (BTA) [41], sodium oxalate (SO_x) [42], and phytic acid [43]. However, the effect of organic additives on the voltage response during PEO was still controversial [44–46]. For instance, Zhu et al. [44] reported that the breakdown and final voltages during PEO treatment of AZ31B Mg alloy in electrolytes containing 10 g/L ethylene glycol (EG) and polyethylene glycol (PEG) as organic additives were almost identical to the counterparts obtained in electrolytes without organic additives. The adsorption of these additives by their segments $-\text{CH}_2-\text{CH}_2-\text{O}-$ on the surface of the Mg alloy, with carbon atoms aligned toward the substrate surface and the oxygen atoms oriented toward the electrolyte, was found to have an insignificant effect on the voltage response as compared to the sample without additives. The authors ascribed this result to the high molecular weight of PEG which reduces the adsorption ability of this additive. On the other hand, some organic additives, like ethanol (EtOH) would have no obvious increase in the voltage during PEO. Sun and co-workers [45] also reported that only minor changes in the voltage-time curves of PEO processes conducted in silicate electrolytes without or with an addition of 10 g/L of either halloysite nanotubes (HNT) or BT-loaded HNT. According to Asoh et al. [46], the PEO treatment of AZ31B Mg alloy using a phosphate electrolyte (0.25 M Na_3PO_4) containing 5 vol.% EtOH as an organic additive had no obvious increase in voltage after reaching the value of breakdown voltage (Figure 1a), suggesting that ethanol was not desirable for coating formation presumably due to its somewhat low pH (12.65) and weak base compared with that comprising only Na_3PO_4 (12.73). This result indicated that ethanol could suppress the dissociation of the electrolytes during PEO. In contrast, when other additives, such as GLY and EG, were included in the phosphate electrolyte, the rates of the increase of voltage were higher than when the PEO process was performed in electrolytes without GLY and EG. The electrolyte conductivity would be reduced by the inclusion of alcohol into the Na_3PO_4 -based electrolyte. In other words, the electrolyte resistance could be increased as the addition of EG and GLY led to an increase in the electrolyte viscosity. Microstructural observations revealed that EG or GLY utilized as an additive could act as an enhancer for film qualities, leading to the development of coatings with fewer micropores.

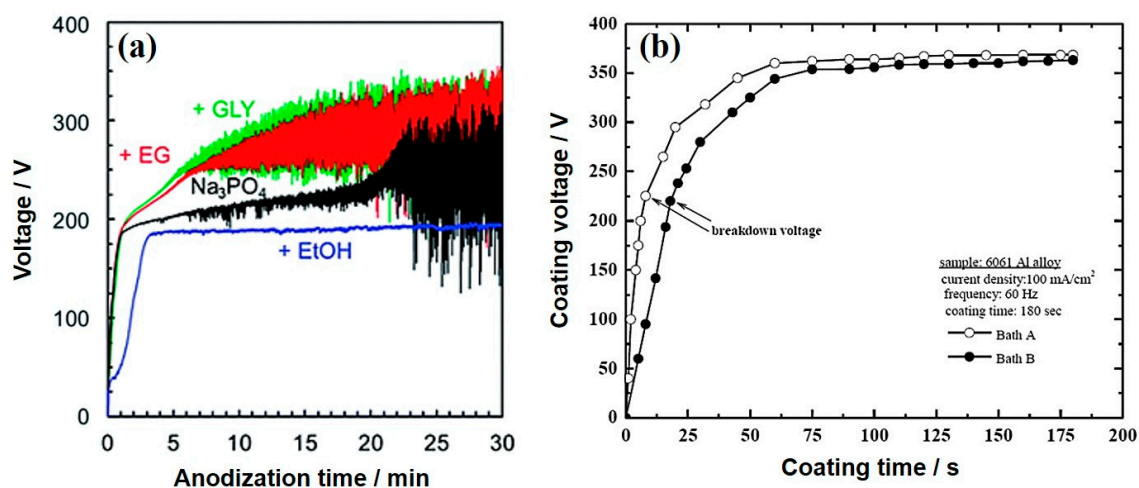


Figure 1. (a) Voltage-time curves of AZ31 Mg alloy coated via plasma electrolytic oxidation (PEO) in electrolytes without and with organic additives, such as ethanol (EtOH), ethylene glycol (EG), and glycerol (GLY). [46] (b) Voltage-time curves of 6061 Al alloy coated in the electrolytes without and with NaBz. Reprinted from permission from [47]. Copyright 2015 Elsevier

Kaseem et al. [47] claimed that the addition of 1 g/L sodium benzoate (NaBz) into the alkaline-aluminate (5.61 KOH + 4.098 g/L NaAlO₂) electrolyte during PEO treatment of 6061 Al alloy would not greatly affect the growth rate and values of breakdown and final voltages as no changes in the electrolyte conductivity have been reported with the inclusion of NaBz into the solution. However, the addition of NaBz into the alkaline-aluminate electrolyte caused a delay in the appearance of plasma discharges, as shown in Figure 1b. It was evident from Figure 1b that a delay in the appearance of plasma discharges can occur during PEO in the electrolyte containing NaBz. Moreover, the voltage in the case of NaBz was slightly lower than that without NaBz. This result was linked to the competition between the dissolution and oxidation of Al alloy substrate in the electrolyte with NaBz [48]. To sum up, the organic additives could affect the characteristics of the PEO process by increasing the voltage. However, controversial results can be found in the literature that are ascribed to differences in the pH, conductivity, concentration, composition, and viscosity of the electrolytes, as well as electrical parameters, used during PEO [1,44–46].

3. Softening Behavior by Organic Additives

The generation of soft plasma discharges usually happens under AC and bipolar current conditions using a higher cathodic current in comparison to the anodic current [1,49–52]. However, several research groups have suggested recently that the inclusion of organic additives into the electrolyte during PEO would help improve the compactness of the coating by facilitating the formation of soft plasma discharges. Such an approach is very simple and does not require sophisticated systems or complex controlling parameters [53]. In this regard, Hussain et al. [54] significantly improved the corrosion resistance of Al–Mg–Si alloy through densification of alumina layer by suppression of intense localized plasma discharges using the dual addition of oxalate and citrate ions to the electrolyte during the PEO treatment of 6061 Al alloy. The base electrolyte was composed of 6 g/L KOH, 4.166 g/L Na₂B₄O₇, while the concentration of oxalate and/or citrate ions was fixed to be 1 g/L. They studied the role of oxalate and citrate ions acting as strong Lewis bases and their interaction with strong Lewis acids of interfacial Al³⁺ ions in the creation of a thick adsorbed electrochemical double layer, which functioned as a barrier layer of complex ligand structures. Such a barrier layer would dissipate the energy of strong plasma discharges, thus, forming a more uniform and homogeneously distributed soft plasma regime that facilitates a thicker, more compact, and dense PEO coating. As the coating time at all experimental conditions was fixed to be 5 min, the decomposition of the adsorbed barrier layer of complex ligand structure under the action of plasma

discharges will dissipate a portion of the discharge energy in breaking their bonds and it will reduce the plasma discharge intensity, thus, facilitating soft plasma formation. The soft plasma conditions, in turn, would facilitate the formation of a thicker, more compact, and dense PEO coating. Their molecular modeling data supported their argument that the coexistence of oxalate and citrate ions facilitated the rapid reformation of the electrical double layer (EDL) because of the competitive adsorption of ions and its molecular orbital interactions. The EDL barrier layer of complex ligand structure had a thick and bulky stern layer and wide concentrated diffuse layer providing higher shielding efficiency and its rapid reformation prevented the substrate to come in direct contact with intensive plasma discharges for a long time, thus the coating is maintained under soft plasma during entire PEO process. By compositional analysis of coating, the study showed that with the decomposition of a barrier layer and its rapid reformation, most of the dissipated heat is encapsulated, which assists slow cooling and induces the formation of a more stable α - Al_2O_3 phase. The slow quenching also helped to maintain lower residual stresses and lower chances of crack formation, which is detrimental to corrosion. Their simple approach with short coating time provided an energy-efficient and cost-effective technique with a higher potential of industrial scalability.

As such, Kamil et al. [55] reported the soft plasma discharges developed in alkaline-silicate-electrolyte-containing complexing agents were useful to optimize the chemical stability and catalytic activity of an Al alloy coated via PEO. Three different complexing agents, such as complexing agents of nitrilotriacetic acid (NTA), ethylenediaminetetraacetic acid (EDTA), and diethylenetriaminepentaacetic acid (DTPA) were added to the alkaline-silicate electrolyte (0.11 M KOH and 0.033 M Na_2SiO_3). The concentration of each complex agent was fixed to be 0.025 M. The results of this work are summarized in Figure 2. As shown in Figure 2a, the voltage-time curves of the Al alloy coated in the alkaline-silicate electrolyte containing NTA, EDTA, and DTPA consisted of three stages whose cell voltages intensify at different rates (Figure 1a), each with a distinctive appearance of plasma discharges (insets). Such variations in the voltage values and plasma discharges led to the formation of coatings with different morphologies, as shown in Figure 2b. The soft plasma discharges developed in the case of DTPA would explain the relatively compact structure observed in Figure 2b. The authors suggested that complexing agents would interact with the Al^{3+} ions by donating electron pairs, strengthening the construction, and accelerate the recovery of the EDL. The rapid formation of EDL was in the order $\text{NTA} > \text{EDTA} > \text{DTPA}$, as shown in Figure 2c. This would maintain a homogeneous electrical field that restrains the destructive effect of plasma discharges by preventing the localization of breakdown spots. Based on the DFT calculations and quantum parameters, they argued that the additive of higher denticity showed a higher fraction of electron transfer (ΔN) and thus experienced higher stability of donor-acceptor interactions, and it ultimately facilitated more favorable adsorption to the interfacial layer. Thus, the DTPA additive generated softer plasma with higher dissipation of plasma discharge energy than the EDTA additive, while on other hand localized intense plasma discharges were observed during PEO coating with the NTA additive. Therefore, coating with NTA additive has a higher porosity and DTPA resulted in a denser and compact coating. Coatings with EDTA and DTPA additives are also rich in stable $\text{Al}_6\text{Si}_2\text{O}_{13}$ phases because of soft plasma formation. The electrochemical impedance spectroscopy (EIS) results of the coatings suggested that the protection capabilities of PEO coatings are directly proportional to the denticity while the catalytic performances are inversely proportional to the denticity of complexing agents used. This is because catalytic performance increases with increasing porosity but corrosion protection decreases. Therefore, both the structural reliability and functional property were obtained together by generating soft plasma using EDTA complexing agent, resulting in a dense coating with dynamic surface topography originated by the activity of plasma discharges, providing the trade-off efficiencies of corrosion protection and catalytic performances.

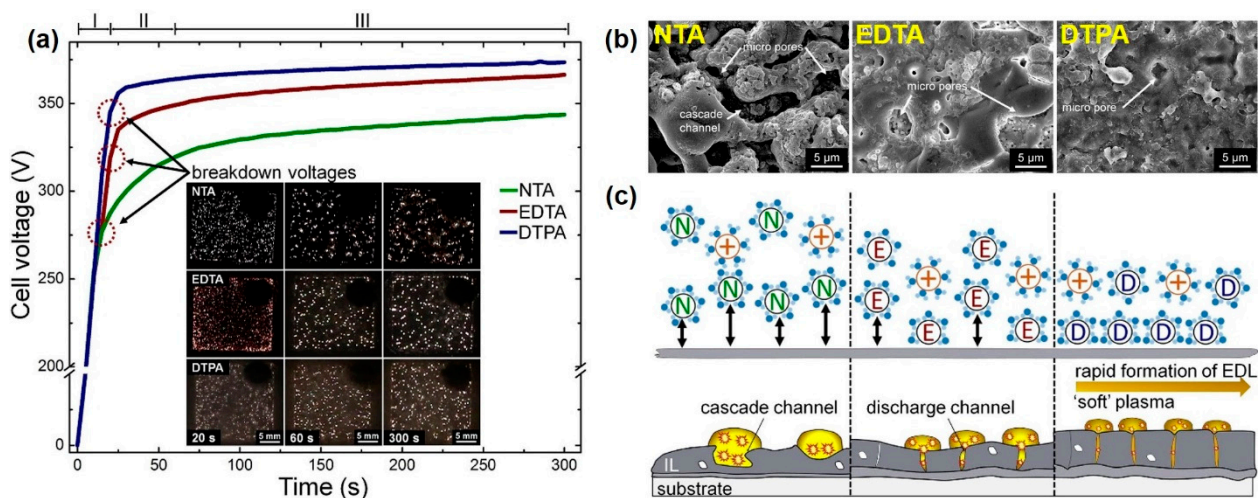


Figure 2. (a) Voltage-time response of the PEO process performed in the alkaline-silicate electrolyte with nitrilotriacetic acid (NTA), ethylenediaminetetraacetic acid (EDTA), and diethylenetriaminepentaacetic acid (DTPA). Insets are the appearance of plasma discharges at the end of stage I (~20 s), stage II (~60 s), and stage III (~300 s). (b) SEM images showing the surface morphologies of the coatings produced in electrolytes with NTA, EDTA, and DTPA. (c) Schematic illustration showing the reconstruction of an electrical double layer (EDL) in electrolytes containing NTA, EDTA, and DTPA and their effects on the generation of soft plasma discharges underlying the formation of PEO coatings. Reprinted from permission from [55]. Copyright 2020 Elsevier.

Wei et. al. [56] claimed that glycerol added into either KF-based electrolyte or phosphate-based electrolyte would affect the evolution of gas products produced during PEO of Zirlo alloy. They reported that the decomposition of glycerol in certain conditions within the plasma discharge channels was believed to be assisted by photo-dissociation, electron impact dissociation, ion impact dissociation, and thermal impact dissociation and is represented by the following equation:



The plasma sparks observed in the KF electrolyte are weak and are further weakened with glycerol addition. The H_2 and O_2 as the only final gases observed in the chromatographs as the weaker plasma sparks could not decompose the glycerol. But the plasma sparks observed in Na_3PO_4 electrolytes are much stronger and intense, which by the addition of glycerol transforms into more uniformly distributed smaller spark discharges. Since the plasma sparks observed were stronger and distributed throughout the anode the final gases consisted of CO peak along with H_2 and O_2 peaks in a chromatograph, which is considered to be the result of decomposed glycerol. As H_2 is generated decomposition of water and GLY, the content of H_2 (53%) produced in KF electrolyte was lower, which further reduced to 21% upon the addition of GLY due to the low intensity of plasma discharges in the electrolyte containing GLY. However, the concentration of H_2 increased to 80.7% due to the strong plasma discharges developed during PEO in the Na_3PO_4 electrolyte. The authors also found that the decomposition of glycerol restricted by the application bipolar current mode would not affect the amount of evolved hydrogen gas, which mainly relied on the intensity of plasma discharges.

As we discussed above, the transition to the soft plasma regime would become easier when the organic additives are included in the electrolyte during PEO. Thus, PEO conducted in electrolytes with organic additives can be regarded as an energy-efficient method if the coating time is reduced without compromising coating quality with this approach. However, further investigation utilizing optical emission spectroscopy would be needed to reveal the mechanisms of the plasma softening, ultimately aiming towards a compact coating layer with functional properties by using organic additives.

4. Influence of Organic Additive on Surface Properties of PEO Coating

4.1. Alcohols and Glycols

Alcohols and glycols are demonstrated to have a considerable influence on the properties of PEO coatings due to their roles in adjusting the electrolyte conductivity and avoiding the occurrence of localized strong plasma discharges. Luo et al. [57] examined the influence of methanol (MeOH) on the characteristics of plasma discharges developed during the PEO coating of Mg alloy. The addition of methanol to the electrolyte helped to reduce the current density during the PEO process and enhanced the uniformity of the coatings. With an increase in the content of MeOH, the amount of dissolved Mg^{2+} ions decreased, which led to an improvement in the compactness and protective properties of the coatings. GLY has been used by several research groups to improve the surface properties of PEO coatings. The influence of GLY concentration (2, 4, 6 mL/L) on the surface properties of AZ91D Mg alloy coated via PEO in Na_2SiO_3 -NaOH- Na_2EDTA electrolyte (base electrolyte) was explored [58]. The concentrations of the base electrolyte components were 10, 2, and 2 g/L for Na_2SiO_3 , NaOH, Na_2EDTA , respectively. The pulse reverse voltage, frequency, and coating time during PEO were controlled to be 400/120 V, 100 Hz, and 15 min, respectively. The addition of GLY into the electrolyte would promote the formation of the small size of intensive plasma discharges. This result was ascribed to the role of GLY in changing the interface between the anode and the electrolyte by its substitution for water molecules, which led to increasing the adsorption capacity of anions. Even though MgO and Mg_2SiO_4 were the main phases of the PEO coating produced in the electrolyte without glycerol, the inclusion of glycerol in the electrolyte help to increase the volume fraction of MgO. Based on potentiodynamic polarization (PDP) assessments in 3.5 wt.% NaCl solution, it was reported that the addition of 4 mL/L of glycerol into the base electrolyte led to a positive shift of corrosion potential (E_{corr}) value from 1.512 V vs. SCE to -1.313 V vs. SCE while the corresponding value of corrosion current density (i_{corr}) for the PEO coating produced in the base electrolyte was reduced from 6.16×10^{-5} to 5.18×10^{-7} A/cm². The highly compact structure with fewer pores and cracks would be the major reason for the lowest corrosion rate in the PEO coatings produced in an electrolyte with 4 mL/L of glycerol.

Pan et al. [59] compared the influence of GLY (5, 10, and 15 g/L) and hydrogen peroxide (H_2O_2) (10, 15, and 20 g/L) added into the base electrolyte composed of ammonium bifluoride (NH_4HF_2) (3, 5, and 7 g/L) during PEO treatment of ZK60 Mg alloy. The compactness and uniformity of the coatings were greatly enhanced upon the inclusion of GLY in the electrolyte. However, the addition of H_2O_2 led to an increase in the surface roughness of the coatings. The corrosion behavior of the coatings obtained in electrolytes without and with additives was examined by the weight loss method after immersion in simulated body fluid solution (SBF) at 36.5 °C for different periods, such as 3, 5, 7, and 9 days. The coatings produced from electrolyte with 5 g/L GLY and 7 g/L NH_4HF_2 exhibited the highest corrosion resistance, which was reflected by a small weight loss of ~2.07%. The addition of higher levels of GLY (10 and 15 g/L) led to the fabrication of coatings with low corrosion resistance. The PEO treatment using an electrolyte system composed of 5 g/L GLY, 10–20 g/L H_2O_2 , 7 g/L NH_4HF_2 caused inferior protective properties of the ZK60 Mg alloy substrate.

The effects of GLY concentration (0, 50, 100, and 200 mL/L) on surface properties of the PEO coatings made on ZK60 Mg alloy were reported by Qiu and co-workers [60]. To discover the influence of GLY on the coating formation, GLY with different contents was added to the base electrolyte composed of 20 g/L Na_2SiO_3 , 7 g/L KOH, and 1 g/L NaF. Based on the molecular dynamics simulations, it was suggested that GLY molecules can be adsorbed at the substrate, which led to a decrease in the number of cracks in the PEO coatings. The model for the adsorbed layer of GLY molecules at the interface is shown in Figure 3. GLY with its functional groups ($-OH$) can lead to specific adsorption at the substrate/electrolyte interface. Thus, it is possible to substitute for the H_2O molecular film formed at the substrate/electrolyte interface in the electrolyte, to some extent, leading to

a reduction in the solid–liquid interfacial tension, as illustrated in Figure 3d. As silicate anions have a similar structure with glycerol because the ionization of silicate ions led to the formation of $\text{SiO}(\text{OH})_3^-$ and $\text{SiO}_2(\text{OH})_2^{2-}$ ions, it was concluded that the intermolecular repulsive force between the interface and silicate ions tended to decrease with adsorption of glycerol molecules. From PDP results in a 3.5 wt.% NaCl solution, it was confirmed that the coating obtained from the electrolyte with 100 mL/L had the highest corrosion resistance in comparison to other samples, which was reflected by the lowest value of i_{corr} with a most positive value of E_{corr} .

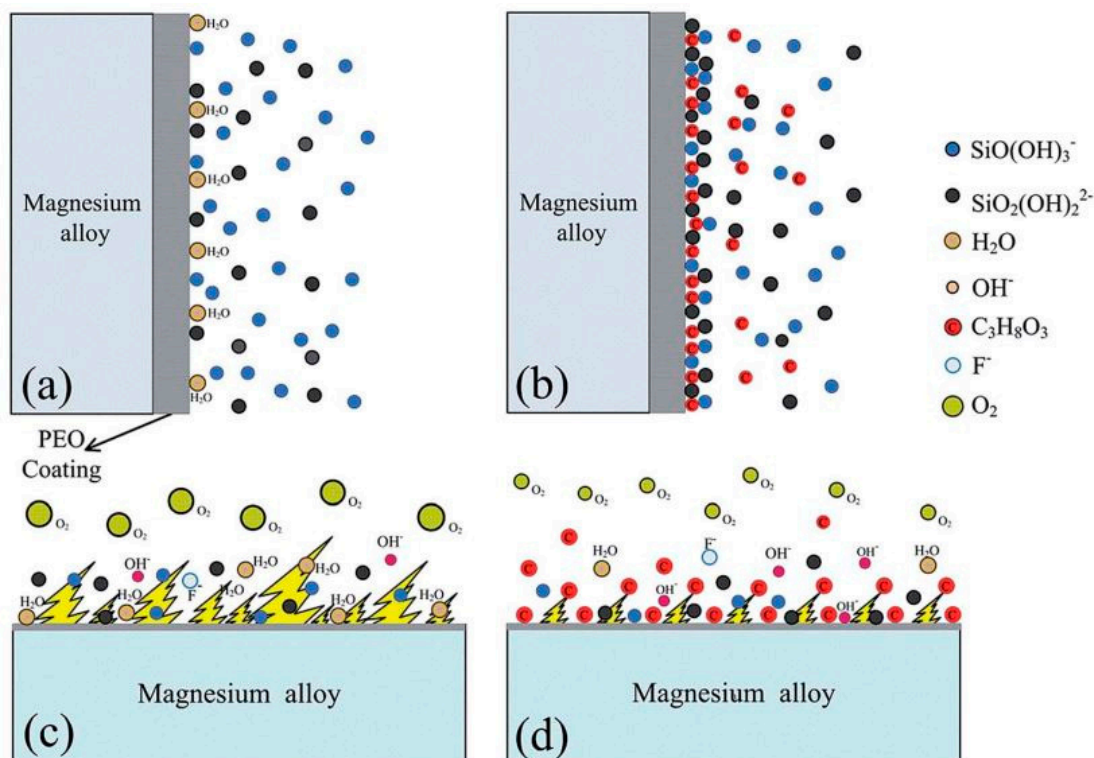


Figure 3. Schematic illustration of the SiO_3^{2-} distribution at anode/electrolyte interface in two different electrolytes at the primary stages of the PEO treatment. (a) In a basic electrolyte, (b) in a basic electrolyte with GLY, (c) discharge mechanism of a basic electrolyte, (d) discharge mechanism of an electrolyte with GLY. Reprinted from permission from [60]. Copyright 2011 Royal Society of Chemistry.

Wang et al. [44] deposited PEO coatings on AZ31B Mg alloy utilizing an electrolyte system composed of 40 g/L NaOH, 50 g/L Na_2SiO_3 , 30 g/L $\text{Na}_2\text{B}_4\text{O}_7$, and 10 g/L $\text{C}_6\text{H}_5\text{O}_7\text{Na}_3$. This electrolyte was modified by adding 10 g/L of EG or its oligomers namely PEG400, PEG1000, and PEG4000. The addition of EG, PEG400, and PEG1000 to the electrolyte resulted in the development of a uniform coating with small micropores. Irrespective of the electrolyte type, MgO, MgSiO_3 , and Mg_2SiO_4 were detected but with different amounts. For example, the PEG1000 enabled the formation of a coating rich in Mg_2SiO_4 . The electrochemical measurements in 3.5 wt.% NaCl solution indicated that the addition of EG to the electrolyte led to an inferior effect on the protective properties of the coatings while the effects of PEG400, PEG1000, and PEG4000 were significant. As the addition of PEG1000 enabled the formation of a relatively compact coating rich in stable Mg_2SiO_4 phase, the coating obtained by this additive had a lower corrosion rate than other coatings.

Alcohols and glycols are well-effective organic additives for improving the protective properties of Mg alloys. Alcohols or glycols that play a dual role in simultaneously enhancing the responding voltage and compactness may be required. For example, the addition of polyglycols with a medium molecular weight can be a suitable candidate to achieve this goal.

4.2. Organic Acids

Phytic acid ($C_6H_{18}O_{24}P_6$) with various concentrations, such as 4, 8, and 12 g/L was added into the alkaline electrolyte (10 g/L NaOH) during the PEO treatment of AZ91 Mg alloy [43]. The current density, frequency, duty cycle, and coating time during PEO were fixed to be 40 mA/cm², 2000 Hz, 20%, and 3 min, respectively. It was found that an increase in the concentration of phytic acid in the solution led to increasing the breakdown voltage, which would be associated with a reduction in the electrolyte conductivity. The corrosion behavior of the PEO coatings was assessed by PDP testes in a 3.5% NaCl as the corrosive medium. The values of E_{corr} and i_{corr} for the coating made in solution with 4 g/L of phytic acid were found to be -1.501 V. vs. SCE and 7.696×10^{-6} A/cm², respectively. These values were changed to -1.470 vs. SCE and 2.559×10^{-6} A/cm² and -1.447 V. vs. SCE and 5.069×10^{-6} A/cm² for the coatings made using 8 or 12 g/L phytic acid, respectively. This result suggested that the coating made in solution with 8 g/L phytic acid had superior corrosion resistance to the counterparts obtained using 4 and 12 g/L phytic acid. Zhang et al. [61] compared the influence of sodium silicate and phytic acid on the surface properties of the PEO coatings of AZ91HP alloy. Here, Si-film describes the coating made in the electrolyte containing 10 g/L NaOH + 18 g/L Na₂SiO₃ while P-film indicates the coating obtained in the electrolyte containing 10 g/L NaOH + 12 g/L phytic acid. Although the Si-film was thicker than the P-film, the pore uniformity of the P-film was better. The composition of the Si-film was amorphous while MgO was the main component in the P-film. PDP tests in 3.5 wt.% NaCl solution revealed that the P-film had a higher corrosion resistance than Si-film, which was attributed to the lowest pore size and better uniformity. In another study, Zhang et al. [62] attributed the improved corrosion resistance of AZ91 Mg alloy, coated via PEO in an alkaline solution containing phytic acid, to the formation of insoluble magnesium phytate.

The influence of terephthalic acid (TPA) on the surface properties of PEO-coated AZ91 Mg alloy was examined by Liu et al. [63,64]. The addition of TPA to the electrolyte led to a reduction in the current density, suppressing the formation of strong plasma discharges. Although the thickness of the coating produced with TPA was slightly lower than the counterparts obtained in the electrolyte without TPA, a smooth and compact coating was obtained when the TPA was added to the electrolyte. For this reason, the coating obtained with TPA had higher corrosion resistance than that obtained without TPA.

As a natural phenolic compound that originates from different plant species, tannic acid ($C_{76}H_{52}O_{46}$) has been widely used in food, medicine, leather, and the chemical industry [65]. Tannic acid ($C_{76}H_{52}O_{46}$) has a good chelating capability with metallic ions (Mg^{2+} and Al^{3+}), forming metal–tannic complexes [33]. Zhang et al. [66] deposited PEO coatings on AZ91 Mg alloy in electrolytes without and with tannic acid. The current density, frequency, duty cycle, and coating time were fixed to be 40 mA/cm², 2000 Hz, 20%, and 3 min, respectively. Three electrolyte systems were prepared. The solution (1) is composed of 10 g/L NaOH and 4 g/L tannic acid. Solution (2) is composed of 10 g/L NaOH and 18 g/L Na₂SiO₃ while solution (3) is composed of 10 g/L NaOH, 18 g/L Na₂SiO₃, and 4 g/L tannic acid. The adsorption of tannic acid on the substrate surface during PEO caused a reduction in the interfacial tension of the gas–liquid and solid–liquid interface, leading to the formation of relatively uniform coatings. The final voltage and coating thickness were found to increase with the addition of tannic acid to the electrolyte. As illustrated in Figure 4a, an insoluble magnesium–tannate complex can be formed at the substrate surface by the reaction between the hydrolysis product of tannic acid with Mg^{2+} ions. The formation of such a complex compound alters the coating color. As shown in Figure 4b, the values of E_{corr} and i_{corr} , determined from PDP tests in 3.5 wt.% NaCl solution, were 1.513 V vs. SCE and 1.226×10^{-5} A/cm², respectively for the coating obtained in the solution (1). While the values of E_{corr} and i_{corr} were found to 1.14 V vs. SCE and 6.125×10^{-7} A/cm², respectively for the coating obtained in the solution (2). Similarly, the values of E_{corr} and i_{corr} were 1.349 V vs. SCE and 1.385×10^{-7} A/cm², respectively for the coating obtained in the solution (3). Based on the above results, it was suggested that the addition of tannic

acid would help to improve the corrosion resistance of the PEO coatings by facilitating the formation of a relatively uniform thick coating by forming of magnesium–tannate complex.

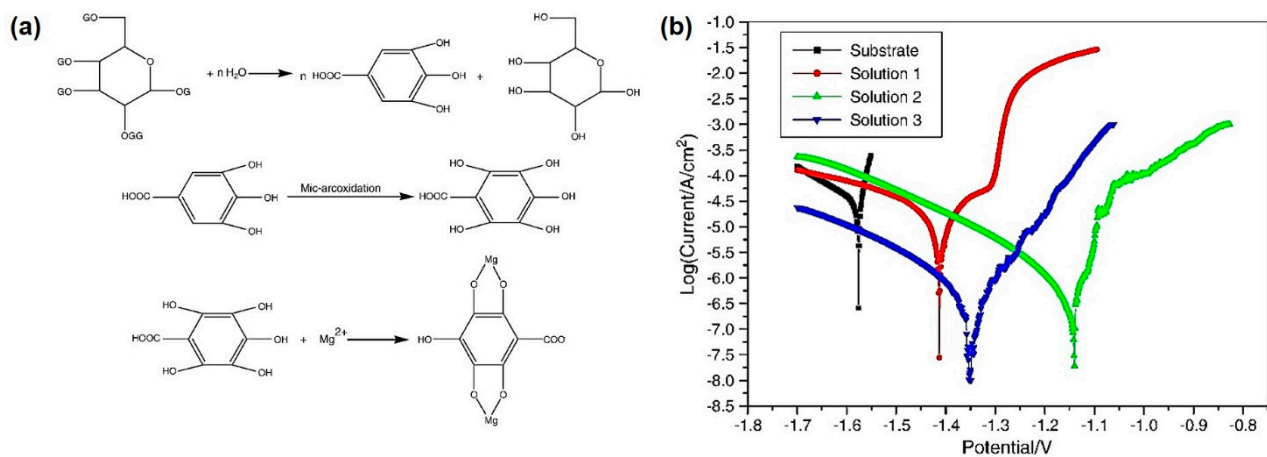


Figure 4. (a) The forming process of Mg alloy in tannic acid during PEO process. (b) potentiodynamic polarization (PDP) results for the coatings obtained in solutions 1, 2, and 3. Reprinted from permission from [66]. Copyright 2012 Elsevier.

Polyaspartic acid (PASP) is another organic additive that has been used as an environment-friendly corrosion inhibitor to protect Mg and its alloys from corrosion [67,68]. The influence of PASP concentration on the surface properties of AZ31 Mg alloy coated via PEO in alkaline-silicate electrolyte without and with various concentrations of PASP, such as 9.6, 19.2, 28.8, and 38.4 g/L was examined by Liu et al. [32]. The alkaline-silicate solution was prepared by mixing 45 g/L NaOH with 100 g/L Na_2SiO_3 . The breakdown voltage and final voltage during PEO treatments were found to increase with the addition of the PASP additive into the alkaline-silicate electrolyte, except in the case of inclusion 38.4 g/L, which did not cause significant changes in values of these parameters. The thickness of the coatings was found to be 6.4, 7.5, 14.6, 23.5, and 16.2 μm for the coatings made in solutions with 0, 9.6, 19.2, 29.8, and 38.4 g/L of PASP, respectively. The differences in the values of cell voltages and thickness of the coatings would be related to the configuration/mode of adsorption. Three different modes, namely *end-on*, *flat-on*, or a combination of *end-on* and *flat-on*, were proposed to describe the adsorption of PASP on the substrate surface during the PEO process (Figure 5a). When the concentration of PASP in the electrolyte was 9.6 g/L, an *end-on* configuration mode was suggested by which PASP adsorbed on the surface of Mg alloy substrate through $-\text{COOH}$ group in the form of ionic or covalent bonds. The *flat-on* mode would be applicable when the 38.4 g/L of PASP was added to the electrolyte, which led to the formation of complex compounds between the Mg alloy and PASP. The combination of *end-on* and *flat-on* modes were proposed in the case of the coatings produced at 19.2 and 29.8 g/L of PASP. This mode was found to be effective due to the formation of uniform and compact coatings as a result of developing low energetic plasma discharges during the PEO process (Figure 5b–g). The coatings produced from electrolytes with PASP were uniform, denser, and thicker than the counterparts produced in the electrolyte without PASP. The addition of PASP promoted the formation of MgO and Mg_2SiO_4 and the amounts of these phases become higher at 19.2 and 29.8 g/L. The polarization resistance (R_p) calculated from PDP tests in 3.5 wt.% NaCl solution was found to be 1.21×10^3 , 1.292×10^3 , 2.81×10^3 , 1.92×10^3 , $1.457 \times 10^4 \Omega \cdot \text{cm}^2$ for the coatings obtained with 0, 9.6, 19.2, 28.8, and 38.4 g/L of PASP, respectively. This result suggested that the coatings obtained in electrolytes with PASP had a lower corrosion rate than those obtained in the electrolyte without PASP.

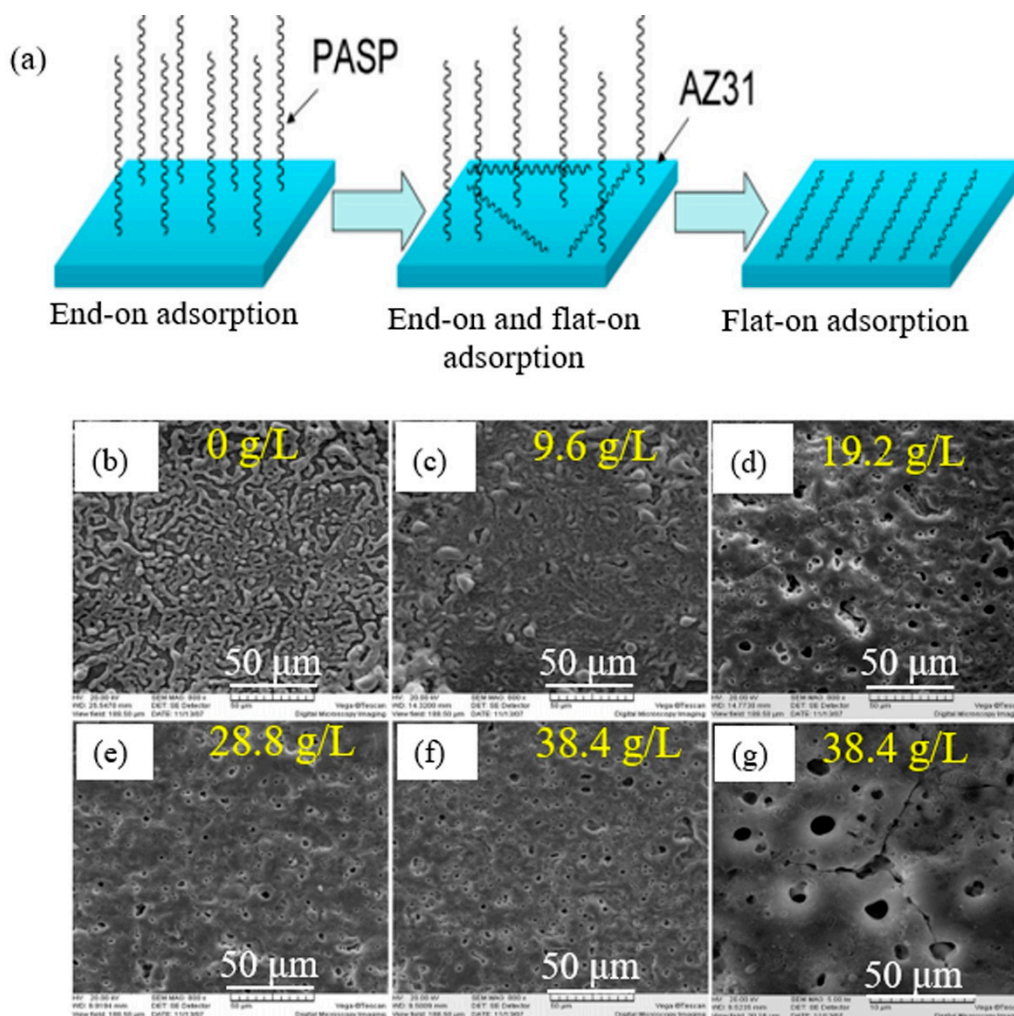


Figure 5. (a) The plausible adsorption configurations modes of polyaspartic acid (PASP) on the substrate surface during PEO. (b–g) The surface morphologies of the coatings obtained in electrolytes with different concentrations of PASP: (b) 0 g/L; (c) 9.6 g/L; (d) 19.2 g/L; (e) 28.8 g/L; (f) and (g) 38.4 g/L. Reprinted from permission from [32]. Copyright 2011 Elsevier.

Ethylenediaminetetraacetic acid (EDTA) was also used as an electrolyte component to protect pure titanium and Mg alloys coated via PEO from corrosion [69,70]. For example, it was reported that the corrosion resistance of the PEO coatings made in a silicate-phosphate electrolyte with EDTA was higher than the counterpart made in a silicate-phosphate electrolyte with sodium tetraborate, which was attributed to the role of EDTA in facilitating the formation of a coating with a smaller pore size [71]. Rogov [72] exploited the inherent properties of EDTA to include various transition metals into the coating layers by reacting either metallic solid or salt with EDTA before PEO.

Among different organic acids used as additives during PEO, the EDTA would be the most promising additive due to the ability of this compound to form relatively stable complex compounds with metallic ions. However, detailed studies on the role of this additive and how the type of metallic cation is linked to EDTA, the effects of the number of protons dissolved from this additive on the pH, and the conductivity of the electrolyte would be needed as these parameters would affect the voltage-time response during PEO.

4.3. Organic Acid Salts

Sodium benzoate, C_6H_5COONa (NaBz), as an expensive eco-friendly organic additive has been utilized in many fields, such as food, medication, and corrosion [47,73]. The addition of the NaBz into the electrolyte during PEO coating was first reported by Liu

et al. [74] who studied the effects of NaBz (0, 0.5, 1, 1.5, 2, 2.5, and 3 g/L) in an alkaline-borate electrolyte on the surface properties of PEO-coated AZ91D Mg alloy. The alkaline-borate electrolyte was composed of 60 g/L NaOH, 25 g/L $\text{Na}_2\text{B}_4\text{O}_7$, and 20 g/L H_3BO_3 . They showed that the addition of NaBz led to a decrease in the pore size and surface roughness. Furthermore, the addition of NaBz led to a significant increase in the corrosion protection of AZ91D films. The authors suggested that Bz^- anions tended to adsorb on the surface of AZ91 Mg alloy during PEO and would combine with Mg^{2+} cations, which led to the formation of monolayer adsorption acting as an effective sparking inhibitor by reducing the intensity of strong plasma discharges. Similarly, Kaseem et al. [47] added 1 g/L NaBz into a base electrolyte composed of 5.61 g/L KOH and 4.098 g/L NaAlO_2 . They reported that the addition of NaBz into the electrolyte during PEO treatment of 6061 Al alloy helped to reduce the average size of micropores, porosity, and surface roughness of the coatings in comparison to the coating obtained in the electrolyte without NaBz. Besides, the compact microstructure obtained in the case of the sample coated with NaBz led to an increase in the amount of $\alpha\text{-Al}_2\text{O}_3$ in the coating because a small surface area was exposed to the electrolyte solution at a slow cooling rate during solidification, which favored the formation of $\alpha\text{-Al}_2\text{O}_3$. During the PEO process, when the sparks are quenched, the electrolyte solution is rushed into the micro-pore as the labyrinth in the coating so that the porous coating had a higher cooling rate due to the solution cooling. For this reason, the coating produced in the electrolyte without NaBz had lower fractions of $\alpha\text{-Al}_2\text{O}_3$, i.e., it had higher fractions of $\gamma\text{-Al}_2\text{O}_3$. The corrosion behavior, evaluated by PDP and EIS tests in 3.5 wt.% NaCl solution indicated that the sample coated with NaBz had lower i_{corr} , higher E_{corr} , and larger impedance than the counterpart coated without NaBz. Therefore, the addition of NaBz to the electrolyte inhibited efficiently the corrosion of the Al alloy substrate.

Sodium oxalate with the formula $\text{Na}_2\text{C}_2\text{O}_4$ (SO_x) could also improve the corrosion resistance of metals through the formation of strong surface complexes inducing the passivation of the metallic surface [75]. As we described in Section 3, the addition of SO_x and SC_i together into the electrolyte improved the compactness of the PEO coating made on 6061 Mg alloys by inducing the formation of soft plasma discharges, which resulted in significant improvements in the corrosion performance of the coatings [54]. Although the addition of SO_x alone improved the corrosion resistance of PEO coating as compared to the case without organic additives, the inclusion of SC_i alone into the electrolyte led to a decrease in the corrosion resistance of the coating when compared to the sample coated without additives. The authors attributed this result to the role of citrate anions in the porosity of the coating by triggering the formation of strong plasma discharges [54].

In another study by Kaseem et al. [42], the porous structure obtained by PEO treatment of 7075 Al alloy in an alkaline-aluminate electrolyte (4 g/L KOH + 3 g/L NaAlO_2) tended to be changed into a compact structure upon addition 1 g/L SO_x into the electrolyte during PEO, which led to a significant decrease of the corrosion rate (Figure 6). However, many cracks have appeared on the surface of the sample coated with SO_x due to the stress developed by filling of the micro-pores as a result of the creation of an oxalate-adsorption layer on the surface of the coatings (Figure 6b). Such cracks were eliminated by further post-treatment in a solution containing oxalate anions (Figure 6c), resulting in a defect-free coating with excellent stability in 3.5 wt.% NaCl solution. Although sodium citrate dihydrate was used to formulate the electrolyte for the PEO process of AZ91 Mg alloy, its role in the morphology, composition, and corrosion behavior of the PEO coating was not reported [76].

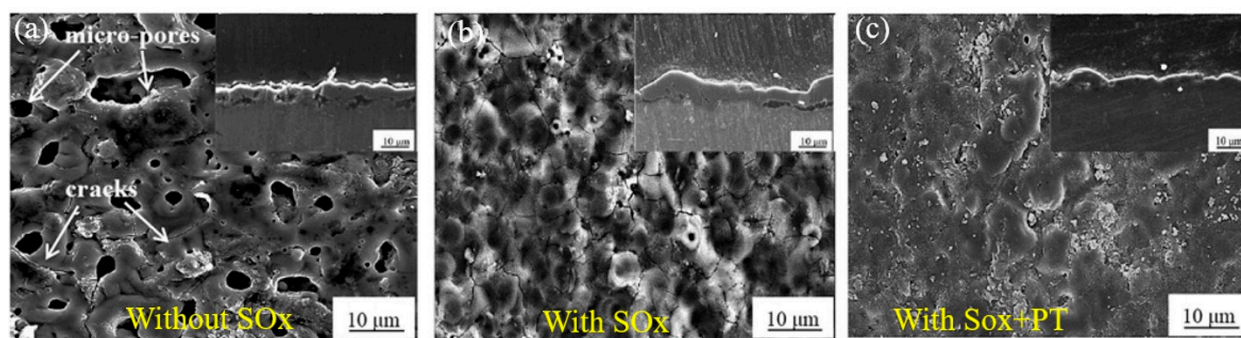


Figure 6. (a,b) SEM images of the PEO coatings produced in an electrolyte without SO_x and with SO_x , respectively. (c) SEM image of the PEO coating produced in the electrolyte with SO_x followed by post-treatment in a SO_x solution. The insets show the corresponding cross-sectional images. Reprinted from permission from [42]. Copyright 2015 Royal Society of Chemistry.

In the work of Wang et al. [77], a complex electrolyte system composed of 13–17 g/L Na_2SiO_3 , 9–15 g/L NaAlO_2 , 2–4 g/L $\text{Na}_2\text{B}_4\text{O}_4$, 1–3 g/L NaOH , 3–7 mL/L GLY, and 3–7 g/L SC_i was developed to improve the corrosion resistance of AZ91D Mg alloy in a 3.5 wt.% NaCl solution. However, the individual role of these additives was not discussed. According to Farhadi et al. [78] potassium stearate ($\text{C}_{18}\text{H}_{35}\text{KO}_2$), prepared by the reaction of pure KOH with pre stearic acid, was dissolved in the electrolyte of PEO coating at 80 °C. Silicon nitride nanoparticles were added also to the electrolyte. The results indicated that the addition of $\text{C}_{18}\text{H}_{35}\text{KO}_2$ into the electrolyte led to an increase in the contact angle to 130° while the corrosion rate of the coating decreased by up to 250-fold. This result was ascribed to the synergism between $\text{C}_{18}\text{H}_{35}\text{KO}_2$ and silicon nitride, which increases the hydrophobicity property of the coating. On the other hand, a mixture of calcium acetate monohydrate and calcium glycerophosphate has been widely used as the base electrolyte during PEO treatment of Ti and Ti alloys as such electrolyte helped to incorporate Ca and P ions, which lead to the formation of hydroxyapatite (HA) in the coating, which is well known to have excellent bioactive properties [69–97].

As the organic salts have the ability not only to improve the corrosion resistance of Mg and Ti alloys but also to incorporate Ca and P elements, the PEO method using electrolyte-containing organic salts is considered a promising strategy for bio-implants owing to the combination of both biocompatible and better corrosion resistance coating.

4.4. Organic Amines

Hexamethylenetetramine (HMT), which is a safe soluble amine, was extensively employed during the PEO treatment of Mg [98–100]. For example, Bai and Chen [99] examined the influence of sodium borate (0.1 M) and HMT (0.1 M) as additives on the morphology and corrosion behavior of PEO coatings made on AZ91D Mg alloy utilizing an electrolyte composed of 1.5 M KOH, 0.04 M sodium citrate, 0.1 M H_3PO_4 , and 0.08 M Na_2SiO_3 . It was found that both additives led to a decrease in the breakdown voltage, pore size, and surface roughness of the coatings. The ability of HMT to reduce the thermal stress during the solidification of molten oxides led to the removal of cracks from the PEO-coated samples. In contrast, sodium borate only caused a slight change in the structure and composition of the PEO coatings. As a result, PDP tests in 5 wt.% NaCl solution indicated that both additives helped to improve the protective properties of PEO coatings. Gozuacik et al. [100] reported an increase in the pore size after the inclusion of HMT (2 g/L) into an alkaline silicate-fluoride solution (2 g/L KOH+ 1g/L KF+ 1.85 g/L Na_2SiO_3) during the PEO treatment of AZ91 Mg-alloy, accompanied by a reduction in the thickness of the coatings obtained in the solution without HMT. Echeverry-Rendon and co-workers [101] compared the corrosion behavior of pure magnesium coated via PEO utilizing alkaline-silicate electrolytes (0.07 M KOH + 0.1 M Na_2SiO_3) without and with separate addition of 0.2 M NaF, 0.05 M mannitol (MAN), and 0.07 M HMT. Figure 7a indicated that the addition of NaF to the alkaline-silicate electrolyte increases the electrolyte conductivity and reduces

the intensity of plasma discharges, resulting in the formation of a compact coating on the surface of pure magnesium. In contrast, both organic additives resulted in the development of porous coating due to the gas evolved at the electrolyte-coating interface (Figure 7b,c). Such a porous structure is expected to facilitate the penetration of corrosive species through the PEO coating reaching the metallic substrate. The thickness of the coating was affected by the applied current density during PEO where the highest value of the thickness of $\sim 12 \mu\text{m}$ was obtained in the sample treated in the electrolyte with HMT at a current density of $\sim 167 \text{ mA}/\text{cm}^2$. Echeverry-Rendon et al. [102] in another work reported that the two-step PEO treatment of pure Mg with HMT or MAN would lead to considerable improvements in the corrosion resistance for biomedical applications.

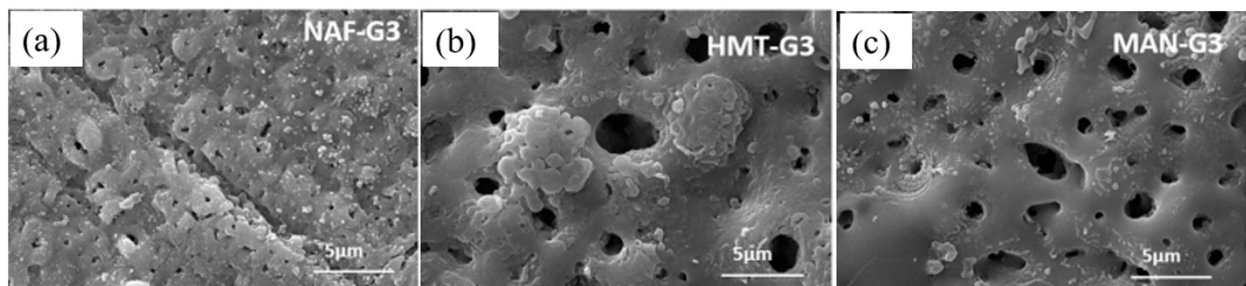


Figure 7. (a–c) SEM images of the PEO coatings made on pure magnesium from electrolyte (a) with NaF, (b) with hexamethylenetetramine (HMT), and (c) with mannitol (MAN). Reprinted from permission from [101]. Copyright 2018 Elsevier.

To improve the electrochemical stability of AZ31 Mg alloy, Pak et al. [38] added separately 0.02 M of APTMS, TEA, and GLY additives into the alkaline-silicate-fluoride electrolyte (3 g/L NaOH + 10 g/L Na_2SiO_3 + 1 g/L NaF) during PEO, and the results were compared to the case with no organic additives. Here, M-Coat refers to the sample coated in the alkaline-silicate-fluoride without additives while G-coat, T-coat, and A-coat describe the samples coated in the electrolyte with GLY, TEA, and APTMS, respectively. The coatings were mainly composed of MgO and Mg_2SiO_4 , which indicated that the influence of organic additives on the composition of the coatings was insignificant. The A-coat sample had higher corrosion resistance than the T-coat and G-coat samples, which was attributed to the formation of a more uniform and compact coating with an Mg–O–Si bond with long aminopropyl chains. Although the pore size and crack levels in the T-coat sample were higher than that of G-Coat, the corrosion resistance of the coating with TEA was higher than that with GLY due to the higher thickness. In the work of Cai et al. [103], TEA was added to the electrolyte used during the PEO process of AZ91 Mg alloy. However, the role of TEA in this work was not discussed. The addition of tris(hydroxymethyl)aminomethane ($\text{HOCH}_2)_3\text{CNH}_2$ into the alkaline-phosphate electrolyte during the PEO coating of titanium led to significant improvements in the protective properties in comparison to the untreated substrate or the coatings produced in the alkaline-phosphate electrolyte, with other additives, such as sodium sulfate, di-ammonium hydrogen phosphate, and ammonium acetate. This result was attributed to the role of the tris(hydroxymethyl)aminomethane additive in developing a less porous coating with a high content of the rutile phase. Tris(hydroxymethyl)aminomethane ($\text{C}_4\text{H}_{11}\text{NO}_3$) into the alkaline-phosphate electrolyte during the PEO coating of titanium led to significant improvements in the protective properties in comparison to the untreated substrate or the coatings produced in the alkaline-phosphate electrolyte, with other additives, such as sodium sulfate, di-ammonium hydrogen phosphate, and ammonium acetate. This result was attributed to the role of the tris(hydroxymethyl)aminomethane additive in developing a less porous coating with a high content of the rutile phase.

Considering the low toxicity of the organic amines and their positive effects on the corrosion resistance of Mg alloys, these additives could be used for the modification of Mg

alloy implants in biomedical fields. However, more studies must be done to explore the bioactive properties of the metallic alloys coated in electrolytes containing organic amines.

4.5. Aromatic Compounds

Aromatic additives usually improve the density of the coatings by slowing the reaction rate of metallic substrate and oxygen during the oxidation process, which makes the coating grow slowly and stably. One of the aromatic compounds that worked as a corrosion inhibitor of metals is 8-hydroxyquinoline (8-HQ). The ability of 8-HQ to form a stable complex of $\text{Mg}(\text{HQ})_2$ with Mg^{2+} ions was exploited by several research groups to design a new electrolyte system for PEO coatings. According to Zhang et al. [104], a series of PEO coatings was prepared on AZ91 Mg alloy by utilizing an alkaline-silicate electrolyte without and with the addition of various concentrations 8-HQ, such as 2, 5, and 8 g/L. The current density, frequency, duty cycle, and coating time during PEO treatments were adjusted to be 40 mA/cm², 2000 Hz, 20%, and 3 min, respectively. The addition of 8HQ into silicate solution during PEO decreased the electrolyte conductivity and promoted coating formation [104]. The addition of this additive to the PEO electrolyte led to the formation of insoluble $\text{Mg}(\text{HQ})_2$ and a decrease in pore size. An increase in the final voltage accompanied by the formation of strong plasma discharges was observed when the content of 8-HQ was increased from 2 to 8 g/L. Such strong plasma discharges would induce the formation of MgAl_2O_4 through the reaction between MgO and Al_2O_3 . Thus, MgO, Mg_2SiO_4 , and MgAl_2O_4 were the main phases in the coating produced with 5 g/L 8-HQ while Mg_2SiO_4 and MgAl_2O_4 were the compositions of the coating obtained with 8 g/L 8-HQ, which showed a decrease in the thickness. The homogeneity of the coatings was improved when PEO was performed in the electrolyte with 2g/L 8-HQ, which helped to reduce the size of micropores. In contrast, heterogeneous coatings were obtained by PEO treatment in electrolytes with 5 and 8 g/L 8-HQ. The corrosion behavior of the coatings obtained in electrolytes containing 0, 2, 5, and 8 g/L 8-HQ was examined by PDP tests in a 3.5% NaCl solution. The electrochemical parameters namely E_{corr} and i_{corr} for the coating obtained in the alkaline-silicate electrolyte without 8-HQ were calculated to be -1.528 V vs. SCE and 40.0 $\mu\text{A}/\text{cm}^2$, respectively. The addition of 2 g/L of 8-HQ to the electrolyte led to the formation of the most protective coating with values of -1.480 V vs. SCE and 2.2 $\mu\text{A}/\text{cm}^2$ for E_{corr} and i_{corr} , respectively. Although the addition of 5 and 8 g/L of 8-HQ coating led to an increase in the corrosion resistance of PEO coatings in comparison to that obtained in the electrolyte without 8-HQ, their effects on the corrosion resistance were less when compared to the coating obtained with 2 g/L of 8-HQ. The improved corrosion resistance in the coating obtained with 2 g/L of 8-HQ was attributed to the uniform, compact structure with less porosity, which prevented the corrosive species from reaching the substrate.

Guo et al. [41] examined the impacts of benzotriazole (BTA) on the coating properties of the PEO-coated AZ31B Mg alloy. The base electrolyte is composed of 60 g/L KOH, 70 g/L Na_2SiO_3 , 60 g/L $\text{Na}_2\text{B}_4\text{O}_7$, and 30 g/L Na_2CO_3 while the concentration of BTA added to the base electrolyte was varied to be 0, 3, 5, and 10 g/L. The results indicated that a BTA adsorption layer tended to be created on the substrate surface. The variations in the concentration of BTA (0, 3, 5, and 10 g/L) during PEO led to significant changes in the surface properties of the coatings. However, the coating produced with 5 g/L BTA exhibited superior corrosion resistance to other coatings, which was linked to the fact that the inclusion of 5 g/L BTA to the electrolyte during PEO would induce the formation of a compact and thick coating. Recently, Kaseem et al. [105] reported that designing an electrolyte system composed of 5 g/L BTA and 5 g/L phosphate ions led to great enhancements in the electrochemical stability of PEO coatings made on Al alloy.

Based on the successful utilization of 8-HQ and BTA as organic inhibitors during PEO treatment of Mg alloys, one can think of other types of aromatic inhibitors that are more environmentally friendly, with better corrosion performance and the ability to form stable complexes with metallic ions, compared to 8-HQ and BTA. Finding new inhibitors

containing aromatic groups would facilitate the transition to the soft plasma regime and, in turn, compact coatings with better protective properties can be developed.

4.6. Carbohydrate Compounds

Starch is a natural and non-toxic substance, which consists of two major components: amylose and amylopectin [106]. Since starch contains many –OH functional groups, the inclusion of starch into the electrolyte of the PEO process led to a reduction in the porosity of the coatings by altering the characteristics of plasma discharges. For instance, Kaseem and Ko [39] reported that the corrosion resistance of 6061 Al alloy could be greatly increased by PEO treatment in an alkaline-borate electrolyte (12 g/L NaOH + 9.53 g/L Na₂B₄O₇) with 5 g/L starch. This result was linked to the role of starch in developing a thick compact coating containing a high fraction of α -Al₂O₃, which is well known to have higher chemical stability than γ -Al₂O₃, which is the main phase in the coating obtained in the electrolyte without starch. The formation mechanism of the coatings obtained in the electrolyte without and with starch is shown in Figure 8. As indicated in Figure 8, the adsorption of starch molecules on the substrate surface led to the deposition of a thick jelly layer on the top of the barrier layer that formed during the conventional anodizing stage. During the fixed coating (5 min), the formation of the jelly layer would reduce the intensity of the plasma discharges, which became weaker and uniform, resulting in the formation of a compact coating with fewer structural defects. The role of starch in improving the protective properties of light metals was also examined by Khorasanian et al. [107] who demonstrated that the inclusion of 25 g/L starch into the electrolyte (30 g/L NaCl + 10 g/L NaOH + 25 g/L Na₂SiO₃ + 15 g/L H₂O₂) during PEO treatment of Ti alloy can help to form a thicker and more protective coating compared to that produced in an electrolyte without starch. Furthermore, Fang et al. [40], stated that PEO coating made on AZ31 Mg alloy utilizing an alkaline-silicate-borax electrolyte with starch had a higher corrosion resistance than the counterpart coated in the electrolyte without starch.

Tu et al. [108] studied the protective properties of PEO coating made on AZ31 Mg alloy in an alkaline-silicate-borate electrolyte (45 g/L NaOH, 70 g/L Na₂SiO₃, and 90 g/L Na₂B₄O₇) system without and with 5, 10, 15 g/L sucrose. Regardless of sucrose concentrations, the coatings were composed of MgSiO₃ and Mg₂SiO₄, indicating that sucrose did not affect the composition of the coatings. The morphological results implied that increasing the concentration of sucrose in the electrolyte from 5 to 10 g/L improved the compactness and uniformity of the coatings while the inclusion of 15 g/L of sucrose did not cause a significant change in the morphology of the coatings in comparison to the case when 10 g/L of sucrose was added. As a result, the sample coated with 10 g/L sucrose exhibited the lowest corrosion rate with a low i_{corr} and a high R_p .

Although starch and sucrose have been approved to improve the protective properties of metallic alloys, more studies should be done to understand the complex PEO process in the presence of such additives. For example, understanding the correlation between starch gelatinization and characteristics of the PEO process would be needed. As the electrolyte temperature during PEO would affect the gelatinization phenomenon of starch, carrying out the PEO process in starch electrolytes with different temperatures would be important to understand the role of this additive, which can stabilize the electrolyte solution.

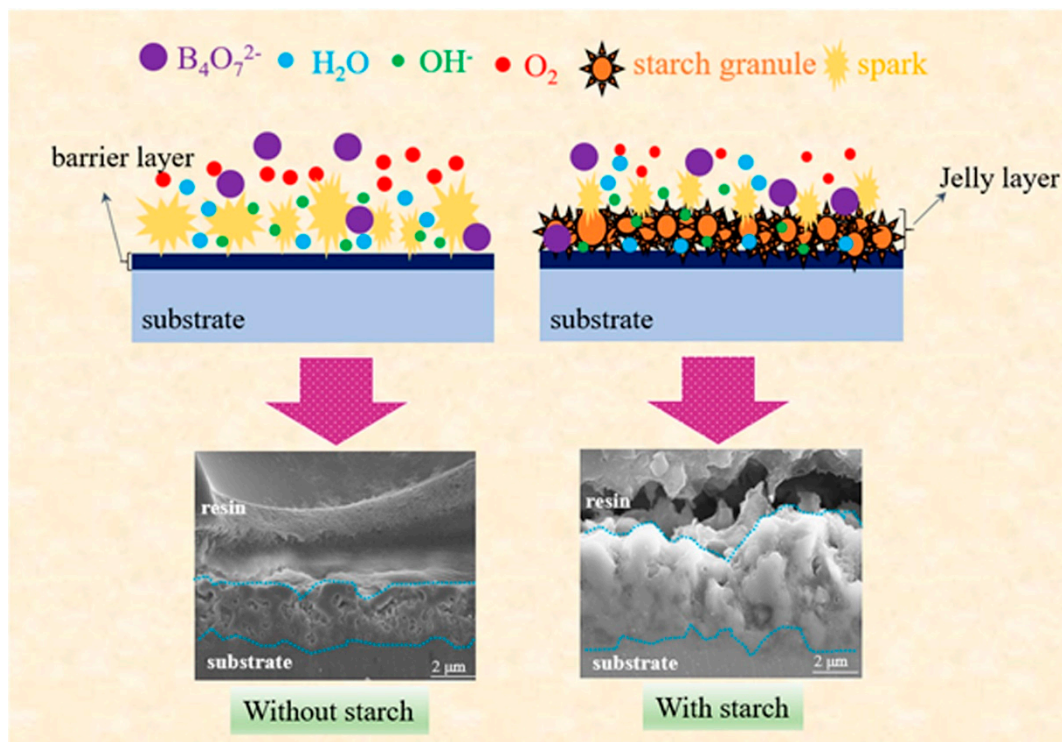


Figure 8. Schematic diagrams showing the formation mechanism for the coatings obtained in an electrolyte without and with starch. A jelly layer was formed in the case of electrolyte-containing starch, leading to generate uniform fine plasma sparks responsible for the formation of a relatively thick layer with fewer structural defects. Reprinted from permission from [39]. Copyright 2019 Elsevier.

4.7. Surfactants

Various types of surfactants can be used during PEO to enhance the quality of the obtained coatings. For example, different surfactants, such as dodecyl sodium sulfate, diphenylamine-4-sulfonic acid sodium, and dodecyl phenyl sodium sulfonate were added to the alkaline-silicate-fluoride-glycerol containing electrolyte during the PEO treatment of AZ31B Mg alloy [109]. In this regard, 0.25 M of surfactants was added to the electrolyte solution composed of 6 g/L Na_2SiO_3 , 2 g/L KF, 2 g/L KOH, and 10 mL/L GLY. As the addition of surfactants did not affect the electrolyte conductivity, no changes in the voltage-time response were reported. During PEO, with the onset of plasma discharges, adsorption of a large number of oxygen molecules and their periodical removal would occur on the substrate surface. The diameter and the adsorption intensity of oxygen bubbles had a considerable impact on the morphology of the coatings. The inclusion of these surfactants alters the interfacial tension, reduces the contact angle and diameter of the oxygen bubbles, and, enables an easy release of oxygen so that the resultant coatings have lower porosity and better quality. Recently, An et al. [110] postulated that the addition of sodium dodecyl sulfate along with TiC and PEG6000 into the electrolyte during the PEO process of AZ91 Mg alloy would enable the formation of a compact coating with improved corrosion resistance. Although the surfactants helped to reduce the size of micropores of the PEO coatings, their effects on the protective properties of PEO coatings and protection mechanism are still undocumented due to the limited number of studies on such compounds in the PEO field.

For a better understanding of the roles of organic compounds added to the electrolyte during PEO treatment, the changes in thickness, surface roughness, sparking behavior, and corrosion resistance in the presence of organic additives are summed up in Table 1. The general conclusion that could be derived from Table 1 is that the addition of organic additives suppressed the strong plasma discharges, reduced the surface roughness, increased

the coating thickness, and improved the protective properties of the PEO coatings made on the metallic substrates and their alloys.

Table 1. Effects of organic additive on the performance of PEO coatings deposited on Mg and its alloys. The influence of organic additives on the properties of PEO coatings made on Al alloys are also presented.

Substrate	Base Electrolyte	Organic Additive	Content	Effect				Ref.
				Thickness	Roughness	Corrosion Resistance	Preventing Sparks	
AZ91 Mg	Silicate	Glycerol	4 mL/L	Dec	Dec	Inc	Yes	[58]
AZ31 Mg	Phosphate	Glycerol	5 mL/L	In	Dec	In	Yes	[46]
ZK60	NH ₄ HF ₂	Glycerol	5–15 mL/L	In	Dec	In	Yes	[59]
ZK60	Alkaline-silicate-fluoride	Glycerol	50–200 mL	In	Un	In	Yes	[60]
Pure Mg	Alkaline-silicate	Mannitol	0.05 M	In	Dec	In	Un	[102]
AZ31 Mg	Silicate-borax	Ethylene glycol	10 g/L	Inc	Dec	Inc	Yes	[44]
AZ91 Mg	Alkaline	Phytic acid	8.0 g/L	Un	Un	In	Yes	[43]
AZ91 Mg	Alkaline-silicate	Phytic acid	12 g/L	Dec	Dec	IN	Yes	[61]
AZ91 Mg	Alkaline	Phytic acid	12 g/L	No change	Un	In	Un	[62]
AZ91 Mg	silicate	Tannic acid	4.0 g/L	Inc	Un	In	Yes	[66]
AZ91 Mg	Alkaline-borate	Terephthalic acid	1–3 g/L	Dec	De	In	Yes	[62,63]
AZ91 Mg	Borate	Terephthalic acid	2 g/L	Un	Un	In	Un	[64]
Mg-Li	Silicate-borax	Aminoacetic acid	6.0 g/L	In	Dec	In	Yes	[111]
AZ31 Mg	silicate	Polyaspartic acid	19.2–28.8 g/L	Un	Dec	In	Yes	[32]
AZ31 Mg	silicate	Citric acid	12 g/L	Un	Dec	In	Yes	[112]
AZ31 Mg	silicate	EDTA	0.03 M	Inc	Un	In	Yes	[113]
6061 Al	Alkaline-silicate	Cu-EDTA	1 g/L	In	Un	In	Yes	[53,55]
ZK60	Silicate-borax	Trisodium citrate	10 g/L	Dec	Un	In	Yes	[114]
AZ40M	phosphate	Ferric citrate	15 g/L	Inc	Un	In	Un	[115]
7075 Al	Alkaline-aluminate	Sodium oxalate	1 g/L	No change	Un	In	Yes	[42]
6061 Al	Alkaline-aluminate	sodium benzoate	1 g/L	No change	Dec	In	Un	[47]
AZ91 Mg	Alkaline- borate	sodium benzoate	1–3 g/L	Dec	Dec	In	Yes	[74]
6061 Al	Alkaline-borate	Sodium oxalate+sodium citrate	1 g/L	In	Dec	In	Yes	[54]
AZ31 Mg	silicate	Sodium citrate	0.5 g/L	Dec	Un	Dec	Yes	[116]
AZ31 Mg	silicate	EDTA-2Na	1 g/L	Dec	Un	Dec	Yes	[116]
AZ31 Mg	silicate	L-Ornithine acetate	0.03 M	In	Un	In	Yes	[117]
AZ91 Mg	borax	Potassium biphthalate	4 g/L	Dec	Dec	In	Yes	[118]
AZ91 Mg	Silicate-phosphate	HMTA	0.1 M	Un	Un	In	Yes	[99]
AZ91 Mg	Alkaline-fluoride-silicate	HMTA	2 and 10 g/L	Dec	Un	In	Yes	[100]
AZ91 Mg	Silicate-borax	Triethanolamine	30 g/L	Un	Dec	In	Yes	[119]
AZ91 Mg	Phosphate	Triethylamine	40–60 g/L	Un	Un	In	Yes	[120, 121]
AZ91 Mg	Phosphate	Diethylenetriamine	0.5 M	Un	Un	In	Yes	[112, 122]
AZ91 Mg	Silicate-phosphate	N,N,N',N'-Tetramethylethylenediamine	0.1 M	Un	Dec	In	Yes	[99]
AZ31 Mg	Silicate	Glucose	10 g/L	In	Dec	In	Yes	[123]
AZ31 Mg	silicate	Sucrose	10 g/L	Un	Dec	In	Yes	[108]
6061 Al	Alkaline-borate	Starch	5 g/L	In	Un	In	Yes	[39]
AZ31 Mg	Alkaline-silicate-borate	Starch	10 g/L	Un	Un	In	Yes	[40]
AZ31 Mg	silicate	Benzotriazole	5 g/L	In	Dec	In	Yes	[41]
6061 Al	Alkaline-silicate-phosphate	Benzotriazole	5 g/L	In	Un	In	Un	[105]
AZ91 Mg	silicate	8-Hydroxyquinoline	2 g/L	In	Un	In	Yes	[104]
AZ31 Mg	Silicate	KH-550 (siloxane)	2 g/L	In	Dec	In	Yes	[124]
AZ31 Mg	Phosphate	polytetrafluoroethylene	18 g/L	Dec	Un	In	No	[125]
AZ31 Mg	Alkaline-silicate-fluoride	Dodecyl sodium sulfate	0.25 g/L	No change	Un	In	Un	[110]

Note: In = increase, De = decrease, Un = un available.

5. Conclusions and Outlook

According to the experimental results highlighted above, it can be stated that the manipulation of the electrolyte composition used during PEO by adding organic additives can provide an effective approach to optimize the surface properties of PEO coatings. Although the main role of organic additives is modifying the morphology of PEO coatings by altering the characteristics of plasma discharges, some changes in the composition of the coatings were reported. Some organic additives affect the voltage-time response during PEO and trigger the fast development of an EDL after disruption by plasma discharges, leading to the formation of compact coatings by facilitating the transition of the soft plasma discharge region. Although organic additives discussed in the present work improved the protective properties of metals to some extent, new additives that are cheaper and more environmentally friendly must be developed. Following the research direction on the addition of organic additives to electrolytes during PEO, future works should aim to improve the compactness of the coating for structural applications and increased the surface area, as well as decorate the matrix of the oxide layer with suitable dopants through the utilization of inorganic electrolytes. Besides, the reaction mechanisms of organic additives during PEO are still underrepresented in the literature and require further study. Moreover, since some research groups studied the effects of organic additives in generating soft plasma discharges, further investigation needs to be carried out to systematically investigate the relationship between the electrolyte species, electrochemical reactions, plasma characteristics, and microstructures of the coatings. Since organic compounds usually have low melting points, their effect might be different from inorganic compounds. Thus, calculations of frontier molecular orbitals should be conducted before the PEO process.

Author Contributions: M.K.: Conceptualization, writing—original draft, writing-review and editing; funding acquisition; B.D.: Sources, writing—review and editing. All authors have read and agreed to the published version of the manuscript.

Funding: This work was supported by the National Research Foundation of Korea (NRF) Grant funded by the Korea government (MSIT) (No. NRF-2019R1G1A1099335).

Institutional Review Board Statement: Not applicable.

Informed Consent Statement: Informed consent was obtained from all subjects involved in the study. The data presented in this study are available on request from the corresponding author.

Data Availability Statement: The data presented in this study are available on request from the corresponding author.

Conflicts of Interest: The authors declare that no conflict of interests.

References

1. Kaseem, M.; Fatimah, S.; Nashrah, N.; Ko, Y.G. Recent progress in surface modification of metals coated by plasma electrolytic oxidation: Principle, structure, and performance. *Prog. Mater. Sci.* **2020**, *117*, 100735. [[CrossRef](#)]
2. Kaseem, M.; Ko, Y.G. Morphological modification and corrosion response of MgO and Mg₃(PO₄)₂ composite formed on magnesium alloy. *Compos. Part B Eng.* **2019**, *176*, 107225. [[CrossRef](#)]
3. Kaseem, M.; Ko, Y.G. A Novel hybrid composite composed of albumin, WO₃, and LDHs film for smart corrosion protection of Mg alloy. *Compos. Part B Eng.* **2021**, *204*, 108490. [[CrossRef](#)]
4. Narayanan, T.S.N.; Song, I.P.; Lee, M.H. Strategies to improve the corrosion resistance of microarc oxidation (MAO) coated magnesium alloys for degradable implants: Prospects and challenges. *Prog. Mater. Sci.* **2014**, *60*, 1–71. [[CrossRef](#)]
5. Li, C.-Y.; Fan, X.-L.; Zeng, R.-C.; Cui, L.-Y.; Li, S.-Q.; Zhang, F.; He, Q.-K.; Kannan, M.B.; Jiang, H.-W.; Chen, D.-C.; et al. Corrosion resistance of in-situ growth of nano-sized Mg(OH)₂ on micro-arc oxidized magnesium alloy AZ31—Influence of EDTA. *J. Mater. Sci. Technol.* **2019**, *35*, 1088–1098. [[CrossRef](#)]
6. Kaseem, M.; Hussain, T.; Baek, S.H.; Ko, Y.G. Formation of stable coral reef-like structures via self-assembly of functionalized polyvinyl alcohol for superior corrosion performance of AZ31 Mg alloy. *Mater. Des.* **2020**, *193*, 108823. [[CrossRef](#)]
7. Hussein, R.O.; Nie, X.; Northwood, D.O. An investigation of ceramic coating growth mechanisms in plasma electrolytic oxidation (PEO) processing. *Electrochim. Acta* **2013**, *112*, 111–119. [[CrossRef](#)]

8. Curran, J.A.; Kalkanci, H.; Magurova, Y.; Clyne, T.W. Mullite-rich plasma electrolytic oxide coatings for thermal barrier applications. *Surf. Coat. Technol.* **2007**, *201*, 8683–8687. [[CrossRef](#)]
9. Kaseem, M.; Ko, Y.G. Electrochemical response of Al₂O₃–MoO₂–TiO₂ oxide films formed on 6061 Al alloy by plasma electrolytic oxidation. *J. Electrochem. Soc.* **2016**, *163*, C587–C592. [[CrossRef](#)]
10. Su, P.; Wu, X.; Jiang, Z.; Guo, Y. Effects of working frequency on the structure and corrosion resistance of plasma electrolytic oxidation coatings formed on a ZK60 Mg alloy. *Int. J. Appl. Ceram. Technol.* **2009**, *8*, 112–119.
11. Kaseem, M.; Kamil, M.; Ko, Y. Electrochemical response of MoO₂–Al₂O₃ oxide films via plasma electrolytic oxidation. *Surf. Coat. Technol.* **2017**, *322*, 163–173. [[CrossRef](#)]
12. Songur, F.; Dikici, B.; Niinomi, M.; Arslan, E. The plasma electrolytic oxidation (PEO) coatings to enhance in-vitro corrosion resistance of Ti–29Nb–13Ta–4.6Zr alloys: The combined effect of duty cycle and the deposition frequency. *Surf. Coat. Technol.* **2019**, *374*, 345–354. [[CrossRef](#)]
13. Hussein, R.; Zhang, P.; Nie, X.; Xia, Y.; Northwood, D. The effect of current mode and discharge type on the corrosion resistance of plasma electrolytic oxidation (PEO) coated magnesium alloy AJ62. *Surf. Coat. Technol.* **2011**, *206*, 1990–1997. [[CrossRef](#)]
14. Kaseem, M.; Kim, M.J.; Ko, Y.G. Hydration-dehydration behavior induced densification of porous plasma electrolysis coating. *J. Alloys Compd.* **2019**, *798*, 220–226. [[CrossRef](#)]
15. Kaseem, M.; Ko, Y.G. Benzoate intercalated Mg–Al-layered double hydroxides (LDHs) as efficient chloride traps for plasma electrolysis coatings. *J. Alloys Compd.* **2019**, *787*, 772–778. [[CrossRef](#)]
16. Kaseem, M.; min, J.H.; Ko, Y.G. Corrosion behavior of Al-1 wt.% Mg-0.85 wt.%Si alloy coated by micro-arc-oxidation using TiO₂ and Na₂MoO₄ additives: Role of current density. *J. Alloys Compd.* **2017**, *723*, 448–455.
17. Kaseem, M.; Yang, H.W.; Ko, Y.G. Toward a nearly defect-free coating via high-energy plasma sparks. *Sci. Rep.* **2017**, *7*, 1–10. [[CrossRef](#)]
18. Srinivasan, P.B.; Liang, J.; Blawert, C.; Störmer, M.; Dietzel, W. Effect of current density on the microstructure and corrosion behaviour of plasma electrolytic oxidation treated AM50 magnesium alloy. *Appl. Surf. Sci.* **2009**, *255*, 4212–4218. [[CrossRef](#)]
19. Vakili-Azghandi, M.; Fattah-Alhosseini, A. Effects of duty cycle, current frequency, and current density on corrosion behavior of the plasma electrolytic oxidation coatings on 6061 Al alloy in artificial seawater. *Met. Mater. Trans. A* **2017**, *48*, 4681–4692. [[CrossRef](#)]
20. Fattah-Alhosseini, A.; Keshavarz, M.K.; Molaei, M.; Gashti, S.O. Plasma electrolytic oxidation (PEO) process on commercially pure Ti surface: Effects of electrolyte on the microstructure and corrosion behavior of coatings. *Met. Mater. Trans. A* **2018**, *49*, 4966–4979. [[CrossRef](#)]
21. Babaei, K.; Fattah-Alhosseini, A.; Molaei, M. The effects of carbon-based additives on corrosion and wear properties of Plasma electrolytic oxidation (PEO) coatings applied on Aluminum and its alloys: A review. *Surf. Interfaces* **2020**, *21*, 100677. [[CrossRef](#)]
22. Kaseem, M.; Ko, Y.G. On the compactness of the oxide layer induced by utilizing a porosification agent. *Appl. Surf. Sci.* **2019**, *473*, 715–725. [[CrossRef](#)]
23. Kaseem, M.; Ko, Y.G. A novel composite system composed of zirconia and LDHs film grown on plasma electrolysis coating: Toward a stable smart coating. *Ultrason. Sonochem.* **2018**, *49*, 316–324. [[CrossRef](#)]
24. Barati, N.; Yerokhin, A.; Golestanifard, F.; Rastegari, S.; Meletis, E.I. Alumina- zirconia coatings produced by plasma electrolytic oxidation on Al alloy for corrosion resistance improvement. *J. Alloys Compd.* **2017**, *724*, 435–442. [[CrossRef](#)]
25. Fatimah, S.; Kamil, M.; Kwon, J.; Kaseem, M.; Ko, Y. Dual incorporation of SiO₂ and ZrO₂ nanoparticles into the oxide layer on 6061 Al alloy via plasma electrolytic oxidation: Coating structure and corrosion properties. *J. Alloys Compd.* **2017**, *707*, 358–364. [[CrossRef](#)]
26. Kaseem, M.; Lee, Y.H.; Ko, Y.G. Incorporation of MoO₂ and ZrO₂ particles into the oxide film formed on 7075 Al alloy via micro-arc oxidation. *Mater. Lett.* **2016**, *182*, 260–263. [[CrossRef](#)]
27. Darband, G.B.; Aliofkhaezrai, M.; Hamghalam, P.; Valizade, N. Plasma electrolytic oxidation of magnesium and its alloys: Mechanism, properties and applications. *J. Magnes. Alloys* **2017**, *5*, 74–132. [[CrossRef](#)]
28. Clyne, T.W.; Troughton, S.C. A review of recent work on discharge characteristics during plasma electrolytic oxidation of various metals. *Int. Mater. Rev.* **2019**, *64*, 127–162. [[CrossRef](#)]
29. Toorani, M.; Aliofkhaezrai, M. Review of electrochemical properties of hybrid coating systems on Mg with plasma electrolytic oxidation process as pretreatment. *Surf. Interfaces* **2019**, *14*, 262–295. [[CrossRef](#)]
30. Lu, X.; Mohedano, M.; Blawert, C.; Matykina, E.; Arrabal, R.; Kainer, K.U.; Zheludkevich, M.L. Plasma electrolytic oxidation coatings with particle additions—A review. *Surf. Coat. Technol.* **2016**, *307*, 1165–1182. [[CrossRef](#)]
31. Molaei, M.; Nouri, M.; Babaei, K.; Fattah-Alhosseini, A. Improving surface features of PEO coatings on titanium and titanium alloys with zirconia particles: A review. *Surf. Interfaces* **2021**, *22*, 100888. [[CrossRef](#)]
32. Liu, Y.; Zhang, D.; Chen, C.; Zhang, J.; Cui, L. Adsorption orientation of sodium of polyaspartic acid effect on anodic films formed on magnesium alloy. *Appl. Surf. Sci.* **2011**, *257*, 7579–7585. [[CrossRef](#)]
33. Chen, M.; Li, Y.; Lian, J.S.; Jiang, Q. Study of the formation and growth of tannic acid based conversion coating on AZ91D magnesium alloy. *Surf. Coat. Technol.* **2009**, *204*, 736–747. [[CrossRef](#)]
34. Chen, X.; Li, G.; Lian, J.; Jiang, Q. An organic chromium-free conversion coating on AZ91D magnesium alloy. *Appl. Surf. Sci.* **2008**, *255*, 2322–2328. [[CrossRef](#)]

35. Ashassi-Sorkhabi, H.; Ghalebsaz-Jeddi, N.; Hashemzadeh, F.; Jahani, H. Corrosion inhibition of carbon steel in hydrochloric acid by some polyethylene glycols. *Electrochim. Acta* **2006**, *51*, 3848–3854. [[CrossRef](#)]
36. Dou, J.; Chen, Y.; Yu, H.; Chen, C. Research status of magnesium alloys by micro-arc oxidation: A review. *Surf. Eng.* **2017**, *33*, 731–738. [[CrossRef](#)]
37. Zhang, W. Research progress on organic additives in the anodic oxidation process of magnesium and its alloys. *Appl. Mech. Mater.* **2013**, *341–342*, 187–190. [[CrossRef](#)]
38. Pak, S.-N.; Yao, Z.; Ju, K.-S.; Ri, C.-N.; Xia, Q. Effect of organic additives on structure and corrosion resistance of MAO coating. *Vacuum* **2018**, *151*, 8–14. [[CrossRef](#)]
39. Kaseem, M.; Ko, Y.G. Effect of starch on the corrosion behavior of Al–Mg–Si alloy processed by micro arc oxidation from an ecofriendly electrolyte system. *Bioelectrochemistry* **2019**, *128*, 133–139. [[CrossRef](#)]
40. Fang, Y.; Tu, X.; Miao, C.; Xu, Y.; Xie, W.; Chen, F.; Zhang, Y.; Li, J. Effect of starch addition in alkaline electrolyte on the characteristics of plasma electrolytic oxidation coating on AZ31B Mg alloy. *Int. J. Electrochem. Sci.* **2017**, *12*, 11473–11478. [[CrossRef](#)]
41. Guo, X.; An, M.; Yang, P.; Li, H.; Su, C. Effects of benzotriazole on anodized film formed on AZ31B magnesium alloy in environmental-friendly electrolyte. *J. Alloys Compd.* **2009**, *482*, 487–497. [[CrossRef](#)]
42. Kaseem, M.; Kwon, J.H.; Ko, Y.G. Modification of a porous oxide layer formed on an Al–Zn–Mg alloy via plasma electrolytic oxidation and post treatment using oxalate ions. *RSC Adv.* **2016**, *6*, 107109–107113. [[CrossRef](#)]
43. Zhang, R.; Zhang, S.; Duo, S. Influence of phytic acid concentration on coating properties obtained by MAO treatment on magnesium alloys. *Appl. Surf. Sci.* **2009**, *255*, 7893–7897. [[CrossRef](#)]
44. Zhu, F.; Wang, J.; Li, S.; Zhang, J. Preparation and characterization of anodic films on AZ31B Mg alloy formed in the silicate electrolytes with ethylene glycol oligomers as additives. *Appl. Surf. Sci.* **2012**, *258*, 8985–8990. [[CrossRef](#)]
45. Su, M.; Yerokhin, A.; Bychkova, M.Y.; Shtansky, D.V.; Levashov, E.A.; Matthews, A. Self-healing plasma electrolytic oxidation coatings doped with benzotriazole loaded halloysite nanotubes on AM50 magnesium alloy. *Corros. Sci.* **2016**, *111*, 753–769.
46. Asoh, H.; Asakura, K.; Hashimoto, H. Effect of alcohol addition on the structure and corrosion resistance of plasma electrolytic oxidation films formed on AZ31B magnesium alloy. *RSC Adv.* **2020**, *10*, 9026–9036. [[CrossRef](#)]
47. Kaseem, M.; Kamil, M.; Kwon, J.; Ko, Y. Effect of sodium benzoate on corrosion behavior of 6061 Al alloy processed by plasma electrolytic oxidation. *Surf. Coat. Technol.* **2015**, *283*, 268–273. [[CrossRef](#)]
48. Hsu, C.-H.; Teng, H.-P.; Lu, F.-H. Effects of addition of Al(NO₃)₃ to electrolytes on alumina coatings by plasma electrolytic oxidation. *Surf. Coat. Technol.* **2011**, *205*, 3677–3682. [[CrossRef](#)]
49. Sah, S.P.; Tsuji, E.; Aoki, Y.; Habazaki, H. Cathodic pulse breakdown of anodic films on aluminium in alkaline silicate electrolyte—Understanding the role of cathodic half-cycle in AC plasma electrolytic oxidation. *Corros. Sci.* **2012**, *55*, 90–96. [[CrossRef](#)]
50. Tsai, D.-S.; Chen, G.-W.; Chou, C.-C. Probe the micro arc softening phenomenon with pulse transient analysis in plasma electrolytic oxidation. *Surf. Coat. Technol.* **2019**, *357*, 235–243. [[CrossRef](#)]
51. Rogov, A.B.; Yerokhin, A.; Matthews, A. The role of cathodic current in plasma electrolytic oxidation of aluminum: Phenomenological concepts of the “Soft Sparking” Mode. *Langmuir* **2017**, *33*, 11059–11069. [[CrossRef](#)]
52. Tsai, D.-S.; Chou, C.-C. Review of the soft sparking issues in plasma electrolytic oxidation. *Metals* **2018**, *8*, 105. [[CrossRef](#)]
53. Kamil, M.P.; Kaseem, M.; Ko, Y.G. Soft plasma electrolysis with complex ions for optimizing electrochemical performance. *Sci. Rep.* **2017**, *7*, 44458. [[CrossRef](#)] [[PubMed](#)]
54. Hussain, T.; Kaseem, M.; Ko, Y.G. Hard acid–hard base interactions responsible for densification of alumina layer for superior electrochemical performance. *Corros. Sci.* **2020**, *170*, 108663. [[CrossRef](#)]
55. Kamil, M.; Al Zoubi, W.; Yoon, D.; Yang, H.; Ko, Y. Surface modulation of inorganic layer via soft plasma electrolysis for optimizing chemical stability and catalytic activity. *Chem. Eng. J.* **2020**, *391*, 123614. [[CrossRef](#)]
56. Wei, K.; Zhang, Y.; Yu, J.; Liu, R.; Du, J.; Jiang, F.; Xue, W. Analyses of hydrogen release on zirconium alloy anode during plasma electrolytic oxidation. *Mater. Chem. Phys.* **2020**, *251*, 123054. [[CrossRef](#)]
57. Luo, Z.C.; Chen, L.; Yan, Z.C.; Wang, H.L. Effect of Methanol on Plasma Electrolytic Oxidation Process of Mg Alloy. *Corros. Prot.* **2011**, *32*, 448. (In Chinese)
58. Wu, D.; Liu, X.; Lu, K.; Zhang, Y.; Wang, H. Influence of C₃H₈O₃ in the electrolyte on characteristics and corrosion resistance of the microarc oxidation coatings formed on AZ91D magnesium alloy surface. *Appl. Surf. Sci.* **2009**, *255*, 7115–7120. [[CrossRef](#)]
59. Pan, Y.K.; Chen, C.Z.; Wang, D.G.; Yu, X.; Lin, Z.Q. Influence of additives on microstructure and property of microarc oxidized Mg–Si–O coatings. *Ceram. Int.* **2012**, *38*, 5527–5533. [[CrossRef](#)]
60. Qiu, Z.; Zhang, Y.; Li, Y.; Sun, J.; Wang, R.; Wu, X. Glycerol as a leveler on ZK60 magnesium alloys during plasma electrolytic oxidation. *RSC Adv.* **2015**, *5*, 63738–63744. [[CrossRef](#)]
61. Zhang, R.; Xiong, G.; Hu, C. Comparison of coating properties obtained by MAO on magnesium alloys in silicate and phytic acid electrolytes. *Curr. Appl. Phys.* **2010**, *10*, 255–259. [[CrossRef](#)]
62. Zhang, R.; Zhang, S.; Gong, J.; Liu, W.; Zhou, H.; Guo, P.; Wu, X. Properties of anodic coatings obtained in an organic, environmental electrolyte by micro arc oxidation on magnesium alloy. *Adv. Mater. Res.* **2011**, *189–193*, 1001–1004. [[CrossRef](#)]
63. Liu, Y.; Wei, Z.L.; Yang, F.W.; Zhang, Z. Anodizing of AZ91D magnesium alloy in borate-terephthalic acid electrolyte. *Acta Phys. Chim. Sin.* **2011**, *27*, 2385–2392.

64. Liu, Y.; Yang, F.; Zhang, Z.; Zuo, G. Plasma electrolytic oxidation of AZ91D magnesium alloy in biosafety electrolyte for the surgical implant purpose. *Russ. J. Electrochem.* **2013**, *49*, 987–993. [[CrossRef](#)]
65. Kim, T.; Silva, J.; Kim, M.; Jung, Y. Enhanced antioxidant capacity and antimicrobial activity of tannic acid by thermal processing. *Food Chem.* **2010**, *118*, 740–746. [[CrossRef](#)]
66. Zhang, S.; Zhang, R.; Li, W.; Li, M.; Yang, G. Effects of tannic acid on properties of anodic coatings obtained by micro arc oxidation on AZ91 magnesium alloy. *Surf. Coat. Technol.* **2012**, *207*, 170–176. [[CrossRef](#)]
67. Wang, Y.; Wang, J.; Zhang, J.; Zhang, Z. Effects of spark discharge on the anodic coatings on magnesium alloy. *Mater. Lett.* **2006**, *60*, 474–478. [[CrossRef](#)]
68. Yang, L.; Li, Y.; Qian, B.; Hou, B. Polyaspartic acid as a corrosion inhibitor for WE43 magnesium alloy. *J. Magnes. Alloys* **2015**, *3*, 47–51. [[CrossRef](#)]
69. Liao, S.C.; Chang, C.T.; Chen, C.Y.; Lee, C.H.; Lin, W.L. Functionalization of pure titanium MAO coatings by surface modifications for biomedical applications. *Surf. Coat. Technol.* **2020**, *394*, 125812. [[CrossRef](#)]
70. Petrova, E.; Serdechnova, M.; Shulha, T.; Lamaka, S.V.; Wieland, D.C.F.; Karlova, P.; Blawert, C.; Starykevich, M.; Zheludkevich, M.L. Use of synergistic mixture of chelating agents for in situ LDH growth on the surface of PEO-treated AZ91. *Sci. Rep.* **2020**, *10*, 8645. [[CrossRef](#)] [[PubMed](#)]
71. Shi, L.; Xu, Y.; Li, K.; Yao, Z.; Wu, S. Effect of additives on structure and corrosion resistance of ceramic coatings on Mg-Li alloy by micro-arc oxidation. *Curr. Appl. Phys.* **2010**, *10*, 719–723. [[CrossRef](#)]
72. Rogov, A. Plasma electrolytic oxidation of A1050 aluminium alloy in homogeneous silicate-alkaline electrolytes with edta 4–complexes of Fe, Co, Ni, Cu, La and Ba under alternating polarization conditions. *Mater. Chem. Phys.* **2015**, *167*, 136–144. [[CrossRef](#)]
73. Lennerz, B.S.; Vafai, S.B.; Delaney, N.F.; Clish, C.B.; Deik, A.A.; Pierce, K.A.; Ludwig, D.S.; Mootha, V.K. Effects of sodium benzoate, a widely used food preservative, on glucose homeostasis and metabolic profiles in humans. *Mol. Genet. Metab.* **2015**, *114*, 73–79. [[CrossRef](#)]
74. Liu, Y.; Wei, Z.; Yang, F.; Zhang, Z. Environmental friendly anodizing of AZ91D magnesium alloy in alkaline borate–benzoate electrolyte. *J. Alloys Compd.* **2011**, *509*, 6440–6446. [[CrossRef](#)]
75. Kobotiatas, L.; Pebere, N.; Koutsoukos, P.G. Study of the electrochemical behavior of the 7075 aluminum alloy in the presence of sodium oxalate. *Corros. Sci.* **1999**, *41*, 941–957. [[CrossRef](#)]
76. Cao, F.-H.; Cao, J.-L.; Zhang, Z.; Zhang, J.-Q.; Cao, C.-N. Plasma electrolytic oxidation of AZ91D magnesium alloy with different additives and its corrosion behavior. *Mater. Corros.* **2007**, *58*, 696–703. [[CrossRef](#)]
77. Wang, S.-Y.; Xia, Y.-P. Microarc oxidation coating fabricated on AZ91D Mg alloy in an optimized dual electrolyte. *Trans. Nonferrous Met. Soc. China* **2013**, *23*, 412–419. [[CrossRef](#)]
78. Farhadi, S.; Aliofkhazraei, M.; Darband, G.B.; Abolhasani, A.; Rouhaghdam, A.S. Corrosion and wettability of PEO coatings on magnesium by addition of potassium stearate. *J. Magnes. Alloys* **2017**, *5*, 210–216. [[CrossRef](#)]
79. Kang, J.-I.; Son, M.-K.; Choe, H.C.; Brantley, W.A. Bone-like apatite formation on manganese-hydroxyapatite coating formed on Ti–6Al–4V alloy by plasma electrolytic oxidation. *Thin Solid Films* **2016**, *620*, 126–131. [[CrossRef](#)]
80. Hwang, I.-J.; Choe, H.C. Effects of Zn and Si ions on the corrosion behaviors of PEO-treated Ti–6Al–4V alloy. *Appl. Surf. Sci.* **2019**, *477*, 79–90. [[CrossRef](#)]
81. Yu, J.M.; Choe, H.C. Morphology changes and bone formation on PEO-treated Ti6–Al–4V alloy in electrolyte containing Ca, P, Sr, and Si ions. *Appl. Surf. Sci.* **2019**, *477*, 121–130. [[CrossRef](#)]
82. Hwang, I.-J.; Choe, H.C.; Brantley, W.A. Electrochemical characteristics of Ti–6Al–4V after plasma electrolytic oxidation in solutions containing Ca, P, and Zn ions. *Surf. Coat. Technol.* **2017**, *320*, 458–466. [[CrossRef](#)]
83. Kaseem, M.; Choe, H.C. Electrochemical and bioactive characteristics of the porous surface formed on Ti–xNb alloys via plasma electrolytic oxidation. *Surf. Coat. Technol.* **2019**, *378*, 125027. [[CrossRef](#)]
84. Lee, K.; Choe, H.C. Effect of the Mg ion containing oxide films on the biocompatibility of plasma electrolytic oxidized Ti–6Al–4V. *J. Korean Inst. Surf. Eng.* **2016**, *49*, 135–140. [[CrossRef](#)]
85. Kaseem, M.; Choe, H.C. Simultaneous improvement of corrosion resistance and bioactivity of a titanium alloy via wet and dry plasma treatments. *J. Alloys Compd.* **2021**, *851*, 156840. [[CrossRef](#)]
86. Kaseem, M.; Choe, H.C. Triggering the hydroxyapatite deposition on the surface of PEO-coated Ti–6Al–4V alloy via the dual incorporation of Zn and Mg ions. *J. Alloys Compd.* **2020**, *819*, 153038. [[CrossRef](#)]
87. Park, S.Y.; Choe, H.C. Mn-coating on the micro-pore formed Ti–29Nb–xHf alloys by RF-magnetron sputtering for dental applications. *Appl. Surf. Sci.* **2018**, *432*, 278–284. [[CrossRef](#)]
88. Kim, S.P.; Kaseem, M.; Choe, H.C. Plasma electrolytic oxidation of Ti–25Nb–xTa alloys in solution containing Ca and P ions. *Surf. Coat. Technol.* **2020**, *395*, 125916. [[CrossRef](#)]
89. Kim, S.-P.; Cho, H.-R.; Choe, H.-C. Bioactive element coatings on nano-mesh formed Ti–6Al–4V alloy surface using plasma electrolytic oxidation. *Surf. Coat. Technol.* **2021**, *406*, 126649. [[CrossRef](#)]
90. Park, M.-G.; Choe, H.-C. Corrosion behaviors of Zn, Si, and Mn-doped hydroxyapatite coatings formed on the Ti–6Al–4V alloy by plasma electrolytic oxidation. *J. Nanosci. Nanotechnol.* **2020**, *20*, 5618–5624. [[CrossRef](#)]
91. Lim, S.-G.; Choe, H.-C. Bioactive apatite formation on PEO-treated Ti–6Al–4V alloy after 3rd anodic titanium oxidation. *Appl. Surf. Sci.* **2019**, *484*, 365–373. [[CrossRef](#)]

92. Hwang, I.-J.; Choe, H.-C. Surface morphology and cell behavior of Zn-coated Ti-6Al-4V alloy by RF-sputtering after PEO-treatment. *Surf. Coat. Technol.* **2019**, *361*, 386–395. [[CrossRef](#)]
93. Hwang, I.-J.; Choe, H.-C. Hydroxyapatite coatings containing Zn and Si on Ti-6Al-4V alloy by plasma electrolytic oxidation. *Appl. Surf. Sci.* **2018**, *432*, 337–346. [[CrossRef](#)]
94. Kaseem, M.; Choe, H.-C. Acceleration of bone formation and adhesion ability on dental implant surface via plasma electrolytic oxidation in a solution containing bone ions. *Metals* **2021**, *11*, 106. [[CrossRef](#)]
95. Campos, E.M.; Santos-Coquillat, A.; Mingo, B.; Arrabal, R.; Mohedano, M.; Pardo, A.; Ramos, V.; Lacomba, J.-L.L.; Matykina, E. Albumin loaded PEO coatings on Ti—Potential as drug eluting systems. *Surf. Coat. Technol.* **2015**, *283*, 44–51. [[CrossRef](#)]
96. Gnedenkov, S.; Sinebryukhov, S.; Zavidnaya, A.; Egorin, V.; Puz', A.; Mashtalyar, D.; Sergienko, V.; Yerokhin, A.; Matthews, A. Composite hydroxyapatite-PTFE coatings on Mg-Mn-Ce alloy for resorbable implant applications via a plasma electrolytic oxidation-based route. *J. Taiwan Inst. Chem. Eng.* **2014**, *45*, 3104–3109. [[CrossRef](#)]
97. Plekhova, N.G.; Lyapun, I.N.; Drobot, E.I.; Shevchuk, D.V.; Sinebryukhov, S.L.; Mashtalyar, D.V.; Gnedenkov, S.V. Functional state of mesenchymal stem cells upon exposure to bioactive coatings on titanium alloys. *Bull. Exp. Biol. Med.* **2020**, *169*, 147–156. [[CrossRef](#)] [[PubMed](#)]
98. Bai, A. Optimization of anti-corrosion ability of micro-arc oxide coating on AZ91D alloy using experimental strategies. *Surf. Coat. Technol.* **2010**, *204*, 1856–1862. [[CrossRef](#)]
99. Bai, A.; Chen, Z.-J. Effect of electrolyte additives on anti-corrosion ability of micro-arc oxide coatings formed on magnesium alloy AZ91D. *Surf. Coat. Technol.* **2009**, *203*, 1956–1963. [[CrossRef](#)]
100. Gozuacik, N.K.; Altay, M.; Baydogan, M. Micro arc oxidation of AZ91 magnesium alloy—Effect of organic compounds in the electrolyte. *Defect Diffus. Forum* **2014**, *353*, 217–222. [[CrossRef](#)]
101. Echeverry-Rendon, M.; Duque, V.; Quintero, D.; Harmsen, M.C.; Echeverria, F. Novel coatings obtained by plasma electrolytic oxidation to improve the corrosion resistance of magnesium-based biodegradable implants. *Surf. Coat. Technol.* **2018**, *354*, 28–37. [[CrossRef](#)]
102. Echeverry-Rendon, M.; Duque, V.; Quintero, D.; Robledo, S.M.; Harmsen, M.C.; Echeverria, F. Improved corrosion resistance of commercially pure magnesium after its modification by plasma electrolytic oxidation with organic additives. *J. Biomater. Appl.* **2018**, *33*, 725–740. [[CrossRef](#)]
103. Cai, Q.; Wang, L.; Wei, B.; Liu, Q. Electrochemical performance of microarc oxidation films formed on AZ91D magnesium alloy in silicate and phosphate electrolytes. *Surf. Coat. Technol.* **2006**, *200*, 3727–3733. [[CrossRef](#)]
104. Zhang, R.; Zhang, S.; Yang, N.; Yao, L.; He, F.; Zhou, Y.; Xu, X.; Chang, L.; Bai, S. Influence of 8-hydroxyquinoline on properties of anodic coatings obtained by micro arc oxidation on AZ91 magnesium alloys. *J. Alloys Compd.* **2012**, *539*, 249–255. [[CrossRef](#)]
105. Kaseem, M.; Hussain, T.; Ko, Y.G. Tailored alumina coatings for corrosion inhibition considering synergism between phosphate ions and benzotriazole. *J. Alloys Compd.* **2020**, *822*, 153566. [[CrossRef](#)]
106. Corre, D.L.; Coussy, H.A. Preparation and application of starch nanoparticles for nanocomposites: A review. *React. Funct. Polym.* **2014**, *85*, 97–120. [[CrossRef](#)]
107. Khorasanian, M.; Dehghan, A.; Shariat, M.H.; Bahrololoom, M.E.; Javadpour, S. Microstructure and wear resistance of oxide coatings on Ti-6Al-4V produced by plasma electrolytic oxidation in an inexpensive electrolyte. *Surf. Coat. Technol.* **2011**, *206*, 1495–1502. [[CrossRef](#)]
108. Tu, X.; Chen, L.; Shen, J.; Zhang, Y.; Miao, C.; Wu, J. Effects of sucrose on anodized film formed on AZ31B magnesium alloy in environmental-friendly electrolyte. *Int. J. Electrochem. Sci.* **2012**, *7*, 9573–9579.
109. Guo, H.; An, M. Effect of surfactants on surface morphology of ceramic coatings fabricated on magnesium alloys by micro-arc oxidation. *Thin Solid Films* **2006**, *500*, 186–189. [[CrossRef](#)]
110. An, L.; Ma, Y.; Sun, L.; Wang, Z.; Wang, S. Investigation of mutual effects among additives in electrolyte for plasma electrolytic oxidation on magnesium alloys. *J. Magnes. Alloys* **2020**, *8*, 523–536. [[CrossRef](#)]
111. Chang, L.M.; Wang, P.; Liu, C.J. Effects of aminoacetic acid on Mg-Li alloy anodic film. *Electroplat. Poll. Control.* **2010**, *30*, 26–29.
112. Cui, X.; Ping, J. Research progress of microarc oxidation for corrosion prevention of Mg alloys. *J. Chin. Soc. Corros. Prot.* **2018**, *38*, 87.
113. Gou, Y.N.; Zhang, D.F.; Guo, X.X.; Pan, F.S. Influence of ethylene diamine tetraacetic acid on properties of composite anodizing films on AZ31 magnesium alloy. *Trans. Mater. Heat Treat.* **2014**, *35*, 169. [[CrossRef](#)]
114. Lu, S.; Xu, R.Y.; Chen, J.; Hou, Z.D.; Wang, Z.X.; Tang, L. Optimization of silicate electrolyte for micro-arc oxidation and characteristic of coating fabricated on ZK60 magnesium alloy. *Chin. J. Nonferrous Met.* **2010**, *20*, 1868–1875.
115. Feng, L.; Zhang, L.; Li, S.; Zheng, D.; Lin, C.; Dong, S. Effect of ferric citrate on microstructure and corrosion resistance of micro-arc oxidation black film on Mg-alloy AZ40M. *J. Chin. Soc. Corros. Prot.* **2017**, *37*, 360–365.
116. Cui, X.J.; Ping, J.; Dou, B.J.; Fu, Q.X.; Xiu-Zhou, L. Surface morphology and anti-corrosion of micro-arc oxidation coatings prepared in different additives. *China Surf. Eng.* **2018**, *31*, 39–50.
117. Gou, Y.; Zhang, D.; Yi, D.; Zhang, C. Effect of amino acid on the anodic oxidation of magnesium alloy and its mechanism. *Rare Met. Mater. Eng.* **2017**, *46*, 1103.
118. Liu, Y.; Yang, F.-W.; Wei, Z.-L.; Zhang, Z. Anodizing of AZ91D magnesium alloy using environmental friendly alkaline borate-biphenylate electrolyte. *Trans. Nonferrous Met. Soc. China* **2012**, *22*, 1778–1785. [[CrossRef](#)]

119. Ou, A.; Yu, G.; Hu, B.; He, X.; Jun, Z.; Haibo, Y.; Yen, C. Effect of triethanolamine on anodizing process of magnesium alloys. *CIESC J.* **2009**, *60*, 2118. [[CrossRef](#)]
120. Luo, S.L.; Zhang, T.; Zhou, H.; Chen, J.S. Effect of organic amine on anodizing of magnesium alloys. *Chin. J. Nonferrous Met.* **2004**, *14*, 691.
121. Asoh, H.; Ono, S. Anodizing of magnesium in amine-ethylene glycol electrolyte. *Mater. Sci. Forum.* **2003**, *419*, 957–962. [[CrossRef](#)]
122. Barton, T.F.; Macculloch, J.A.; Ross, P.N. Anodization of magnesium and magnesium based alloys. U.S. Patent 6,280,598, 28 August 2001.
123. Tu, X.H.; Chen, L.; Wu, J.Y. Effect of glucose on properties of anodizing film on AZ31B magnesium alloy. *Chin. J. Nonferrous Met.* **2013**, *23*, 727.
124. Cui, X.; Dai, X.; Zheng, B.; Zhang, Y. Effect of KH-550 content on structure and properties of a micro-arc oxidation coating on Mg alloy AZ31B. *J. Chin. Soc. Corros. Prot.* **2017**, *37*, 227–232.
125. Guo, J.; Wang, L.; Wang, S.C.; Liang, J.; Xue, Q.; Yan, F. Preparation and performance of a novel multifunctional plasma electrolytic oxidation composite coating formed on magnesium alloy. *J. Mater. Sci.* **2009**, *44*, 1998–2006. [[CrossRef](#)]